Department of Precision and Microsystems Engineering

Multibody model-based analysis of a 2 DOF translational mechanism: specifications breakdown from system to sub-system.

Andreu Moliner Brotons

Report no : 2021.094
Coach : Ir. J.W. Spronck & Ir. L. García Rodriguez
Professor : Dr. A. Hunt
Specialisation : Mechatronic System Design (MSD)
Type of report : Design Report
Date : 8 December 2021

Summary

The purpose of the graduation project is to break down specifications for the guiding system of a Reticle masking unit (REMA) of a photolithography scanner.

The structure followed in this summary is the following; first some background about module REMA is presented to show the impact and relevance of the project. Secondly, the specification problem that triggered the graduation project is defined. A model-based approach is presented as a solution for the problem and a multi-body model is chosen as a tool to achieve it. The model is roughly explained to give the reader a visual idea of the system layout. As a conclusion, this approach has shown to have a big impact on the communication and integration between disciplines for the fulfilment of a top level specification.

Aiming to increase the throughput of chip making machines, ASML is constantly increasing the operational speed of its lithography systems. Like in a photography camera, in the ASML machines there is a module responsible for blocking the light from reaching the camera sensor. This module is the reticle masking (REMA) module and its main function is to mask the light from impacting, instead of a camera sensor, the pattern that will be printed on the chip material. The reticle, which holds the pattern, is operated at accelerations 4 times higher than lasts modules, which REMA has to follow.

The accuracy of the printed patterns is directly affected by the positioning of the REMA module end effector. In precision mechanisms, all sources of vibration can be translated into a loss of accuracy due to positioning errors. During REMA operation, inertia forces and torques are generated and exerted to the force frame. These reactions generate vibrations which at the same time induce noise, wear, fatigue and positioning inaccuracies. Moreover, the REMA proximity to the reticle makes it even more critical. In order to prevent these effects due to the reactions generated by the REMA, a specification is defined at a system level.

Due to the complexity of the system, the tracking of certain specifications becomes a challenge during the design process. In the case of the exported reactions specification its analysis is done by one discipline, but the fulfillment of it is affected by many other disciplines. This creates an even more complicated problem, as all the affected clients have to be aware of the specification state in every moment of the design process. A model-based approach is as a multidisciplinary approach with the aim of developing a balanced system solution in response to various stakeholder needs which in the case of this project are dynamics and mechanics disciplines.

This project aims to apply a model-based approach for the REMA module design based on the exported reactions specification. The goal is to study the influence of design parameters in the exported reactions specification in an early development phase and to translate this requirement into smaller design specifications as an input for the sub-module's design. A multi-body model has been selected to do so. This approach would improve the efficiency of the whole design process and increase the first-time-right chances during product development.

Before starting the modelling phase, an investigation on the parasitic disturbances has been performed. In order to generate the model, the REMA module design has been abstracted to an early design stage. Mass, inertia and assembly properties have been kept as in the current system but simplifications and assumptions have been made. Figure 1 (see Figure 48 for the confidential version of the figure), gives an idea of what the model is composed of and its kinematics.

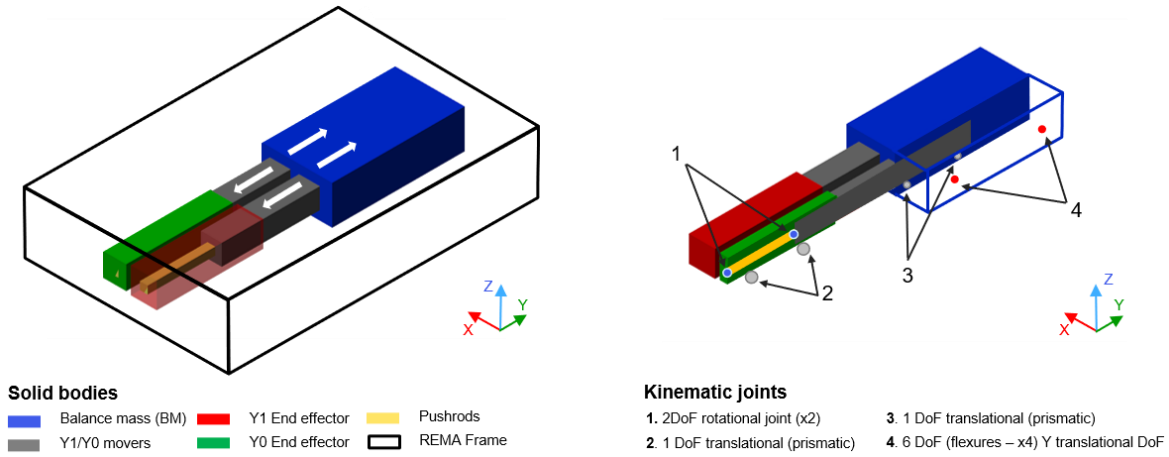

Figure 1. Visual representation of solid bodies and kinematic joints in the model.

The model has a total of two Degrees of Freedom (DOF) corresponding to the Y translational DOF of the two end effectors. Each DOF is controlled by an actuator between the balance mass (BM) and the movers. The BM is suspended by leaf flexures represented by 6DOF joints with a significantly lower stiffness in the Y direction. Consequently, when the actuators exert a force to move the end effector, the same force is exerted on the BM, generating a movement in the opposite direction. After the model has been set up, different analyses have been performed as for example: the effect of the moving mass on the complete exported reactions, the effect of the position of the Center of Gravity (COG) in Y on the BM guiding system loads and the loss of support stiffness of the BM guiding mechanism.

To conclude, the top level exported reaction specification has been broken down into several relevant design parameters. A gravity analysis in the BM and end effector guiding system revealed a non-desired motion of the balance mass. Moreover, the effect of the COG position on the BM guiding systems accentuates this effect generating a positioning error of the end effector.

Overall, awareness has been raised by the results of the project with regards to the traditional linear dynamics analysis. Some of the results obtained by this analysis could not have been found with the current methodology. By the analysis of just one disturbance source via de multibody dynamics model, five different design inputs have been defined. These inputs are of multidisciplinary nature, which shows the power of communication and integration between disciplines that this approach can offer. Analyzing the system as a whole in an abstract and conceptual way helped to understand and gain insight on the root of the analyzed disturbances.

Quite a deep knowledge of the system layout, operation and performance was needed for the realization of this project. As well as, the challenge of having to get used to a complete new software and analysis type. Personally, the project has been a fruitful technical challenge. The most relevant conclusion is the point of view that this approach gives into the importance of the communication between disciplines when having an effect on a common specification. Most of the times this big picture is lost during the design process. This visual and conceptual approach tool, helps to keep that interaction between teams alive during the entire process.

Table of contents

List of figures.

List of acronyms

BM	Balance mass
COG	Center of Gravity
COF	Center of Force
COS	Center of Stiffness
REMA	Reticle Masking
TF	Top Frame
RS	Reticle Stage
WS	Wafer Stage
MF	Metrology Frame
FF	Force Frame
CAD	Computer Aided Design
PoI	Point of interest
CJ	Cylindrical joint

1. Introduction.

Smartphones with more and more capabilities, maintaining its size and a better performance. Computers with more computational power to allow bigger and faster simulations, thinner, lighter. Smart watches, TVs, house appliances... Technology is driving our life. But what is driving technology evolution?
Since 1970, when the first microprocessors were designed, this field has been in a constant change. These processors are the heart of all the devices that we use daily. The number of transistors (smaller devices inside the processor) that can be integrated in a chip, the heat that the chip can dissipate, the number of connections to other devices, are all physical limitations that define the size and final performance of the microprocessors. The most important for the aim of this introduction is the number of transistors that can be put onto one chip. The name of Moore may be familiar to the reader and the well-known Moore's Law. In few words, Moore said that the number of transistors in a dense Integrated Circuit (or chip) will double about every two years. This is not a physical law, but an observation of what he thought would be the trend in technology. After more than 50 years this prediction has become a rule for innovation in electronics design.

There are many factors affecting the number of transistors that is possible to fit onto one chip, but one of the most important is the manufacturing process used to create those transistors. This process involves several steps and technologies but the one of interest for the project is the so called photolithography.

Lithography is basically a process in which a template is copied many times. It consists of several steps and processes but one of them is specifically of interest. This process is the exposure, and consists of five important parts: the light source, the optics, a photoresist material, the mask and the end surface: a silicon wafer.

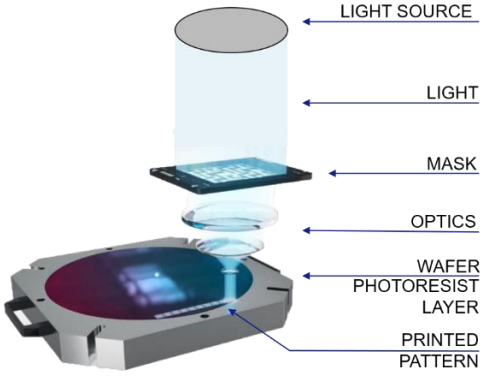

Figure 2. Simplification of lithography process.

The exposure process starts after the silicon wafer has been coated with a photoresist, a light sensitive material. Then, the light is generated and directed to pass through the mask, where the pattern to be copied is placed. After this the light is shaped and it goes into a series of optical lenses and/or mirrors which adjust this shape to print a smaller shape than the mask. Then the desired parts of the light sensitive materials are exposed to this light and a chemical process starts inside the photoresist material. This is a broad overview of what happens inside an ASML lithography machine.

The pattern is printed on the photoresist material and more processes will follow to shape this pattern into a chip. The lithography process directly affects the minimum size that is possible to produce in a chip and thus the number of transistors that can be shaped onto it.

1.1. ASML Lithography.

ASML provides leading patterning solutions that drive the evolution of microchips. Inside this expertise is the photolithography process, in which ASML has been working since its foundation.

The size of the smallest feature that can be printed on a device is driven by the Rayleigh criterion, which is a simple equation that drives and challenges ASML today. ASML has been fighting to reduce this critical dimension since its foundations. Some years ago, a new technology was discovered that allows the wavelength of the light used for the lithography process to be reduced. This technology, called Extreme Ultra Violet or EUV has enabled ASML to produce the smaller feature size so far.

In Figure 48, we can see a layout of an ASML machine. The part of interest for the project is the Reticle Masking Unit (inside the red box), from now on, REMA.

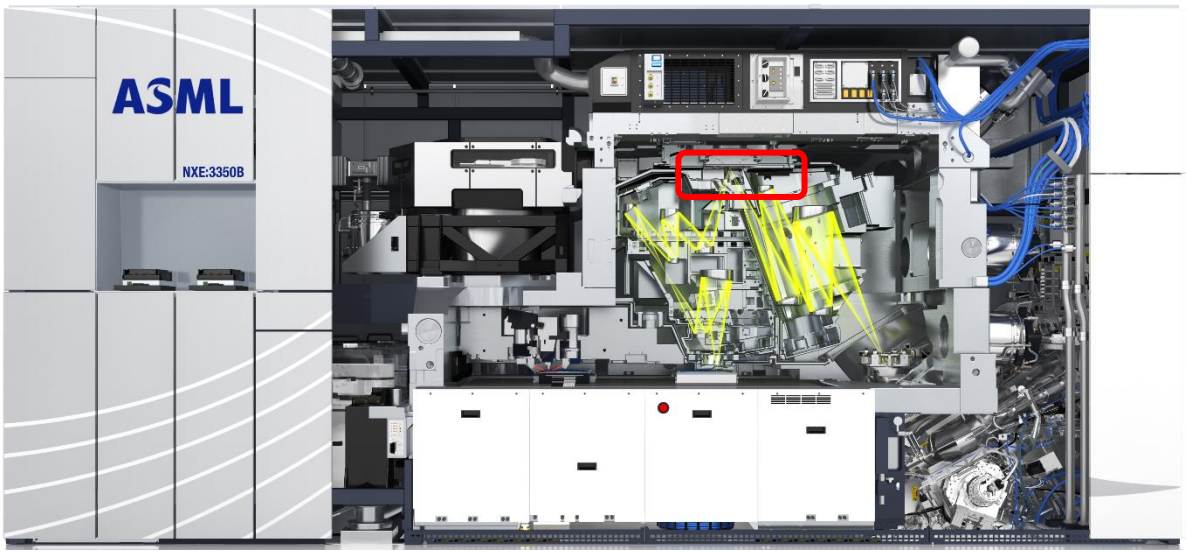

Figure 3. Overview of machine layout.

REMA is located at the top part of the machine, attached to the Top frame (force frame), frame to which the reticle stage is also attached. The reticle stage holds the pattern that is going to be printed on the wafer (the mask), thus its position should be accurately controlled and vibrations or other disturbances should be minimized/eliminated. A vibration or position inaccuracy of the reticle stage could generate, for example, a blurring of the printed shape on the wafer. In a daily example this will be as if when taking a photography, the camera is no stable enough and the picture end up being blurred. In that case, the reticle will be the sensor capturing the image. The fact that the REMA module is attached to the same frame as the reticle stage will be of big importance for the problem definition.

1.2. The Reticle Masking Unit (REMA).

To understand the function of the REMA, it is crucial to know about the exposure technique evolution.

In past lithography machines the mask was exposed in so called steps. In those machines, called steppers, the mask was completely exposed in one go and the pattern printed also in one action, then the wafer moved to a different location and the exposure was repeated (Figure 4, left). New processes appeared and now the EUV machines use a step and scan technology, called scanners. This change in technology changed the function of the REMA module.

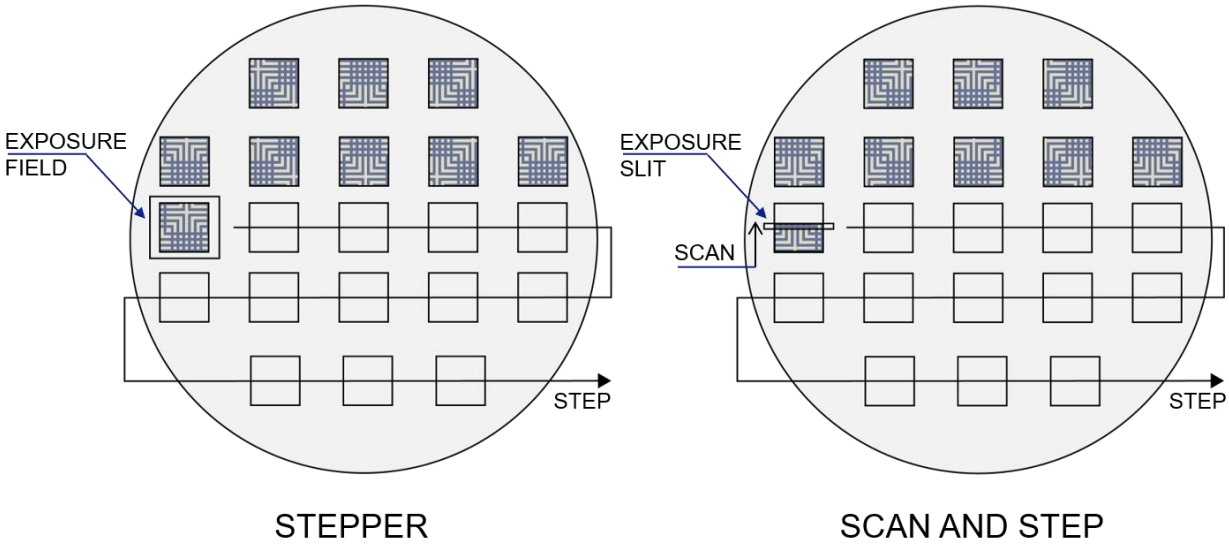

Figure 4. Representation of stepper and scan - step process.

In the scanner process, the light passes through a smaller slit that does not cover the whole size of the mask, but just a portion. A portion of the light passes through that slit (represented in Figure 4 right). Because of that, the reticle has to move along one of its dimensions to expose the whole pattern via this slit, this is called the scan. The function of the REMA in this process is to block the light from reaching undesired parts of the mask. In a stepper, the REMA just needs to cover the edges of the mask and open and close the whole mask when necessary (shutter action). With the step and scan sequence, the REMA needs to open and close when necessary but more importantly, it has to perform a scan sequence following the reticle motion.

In summary, the REMA module must: block light in such a way that only areas of interest within the nominal illuminated area (slit) are exposed, and act as shutter at the start of a scan and during the turnaround phase between two scans.

1.3. Report structure.

To start, Chapter 2 defines the design challenge and problem that triggered this graduation thesis. Chapter 3 goes more into detail on the REMA system. However, most of the information of the REMA system is confidential and it is contained in the confidential Annex. Chapter 4 explains the model generated for the analyses of the system and the assumptions made. Next, Chapter 5 contains the analysis performed via the multibody model and every section concludes with a list of sub-system specifications. Finally, in Chapter 6 & 7 the conclusions and future work recommendations are presented.

Additionally, the confidential Annex contains an extended version of Chapter 3 as well as the overview of the multibody model developed in MATLAB Simscape Multibody.

2. Problem definition.

In this chapter, the problem that started this project is going to be defined and the selected model-based approach explained.

The accuracy of the printed patterns is directly affected by the positioning of the end effector of the REMA module. In precision mechanisms, all source of vibration can be translated into a loss of accuracy due to positioning errors. During REMA operation, inertia forces and torques are generated and exerted to the force frame to which it is attached. These reactions generate vibrations which at the same time induce noise, wear, fatigue and positioning inaccuracies. The REMA module serves as a base for other systems, but it is its proximity to the reticle stage that makes it even more critical. As it can be seen in Figure 5, the REMA module is attached to the force frame (FF) also known as Top Frame). This frame, as the name sates, is the frame carrying the forces generated by the modules and it is isolated from the metrology frame (MF), responsible for measuring the position of the relevant modules. With this separation of frames the errors generated by vibrations coming from the reaction forces of the different mechanisms are not influencing the relevant measurements. However, the reticle stage is attached to the same frame as the REMA. In order to prevent the exported reactions from REMA to affect the reticle stage and other modules attached to the FF, a specification at a system level is defined.

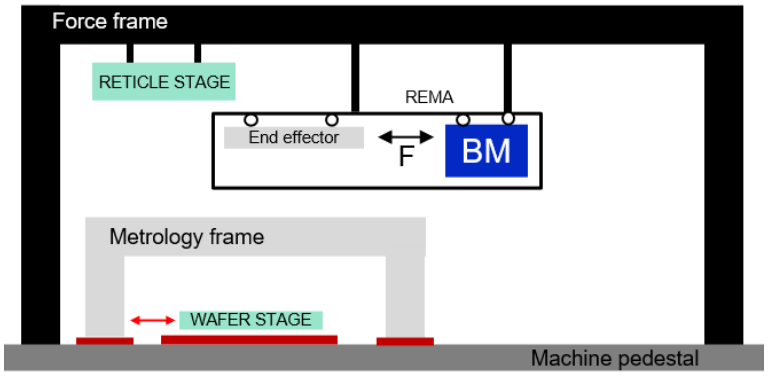

Figure 5. Force and metrology frames

This specification reinforces the fact that in complex mechatronic mechanisms like the REMA module, all sources of vibration can generate an accuracy error. In this case, the source of vibrations are the reactions that could be generated from the REMA module to the force frame, and the errors are all the positioning inaccuracies that this source could generate on other system attached to the same frame (FF). Due to that, the tracking of this specification during the product development gains a lot of importance.

The exported reactions specification involves two main disciplines. Mechanics and dynamics disciplines, divided in mechanical designers and dynamic analysts. The work of both teams is needed to fulfill the requirement. In Figure 6, a simplified workflow of the interaction between these two disciplines is presented.

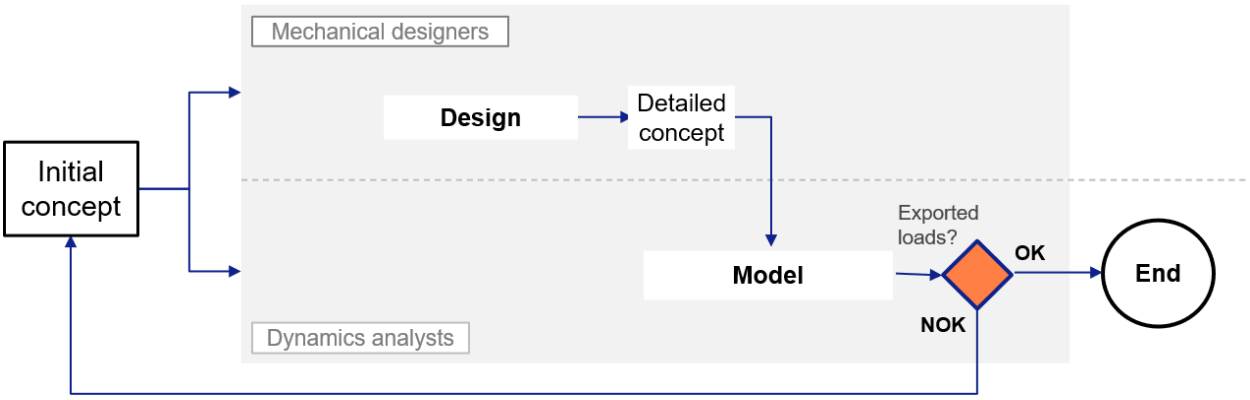

Figure 6. Design flowchart for interaction between disciplines.

The figure represents a design workflow for a product. From left to right, an initial concept is selected and the design process starts with the big gray box. The box is then divided into the two mentioned teams (top/bottom). The mechanical designers start designing a system that fulfills the mechanical specifications coming from the functional requirements, reaching a functional design in the mechanical point of view. On the bottom box, the dynamic analysts are waiting for the detailed design to be finished in order to generate a model and check the top level specifications, like the exported loads. As this specification has not (or barely has) been taken into account during the mechanical design, there is a high chance that it is not fulfilled.

Not fulfilling this specification will make the loop start again applying some changes in the mechanical design or additional dynamic solutions that could have been avoided by an integrated approach. In order to solve this problem, it may seem obvious to include more stages in the dynamic analysts box, to provide the mechanical designers with detailed specifications having an influence in the top level specification. This idea is represented in Figure 7.

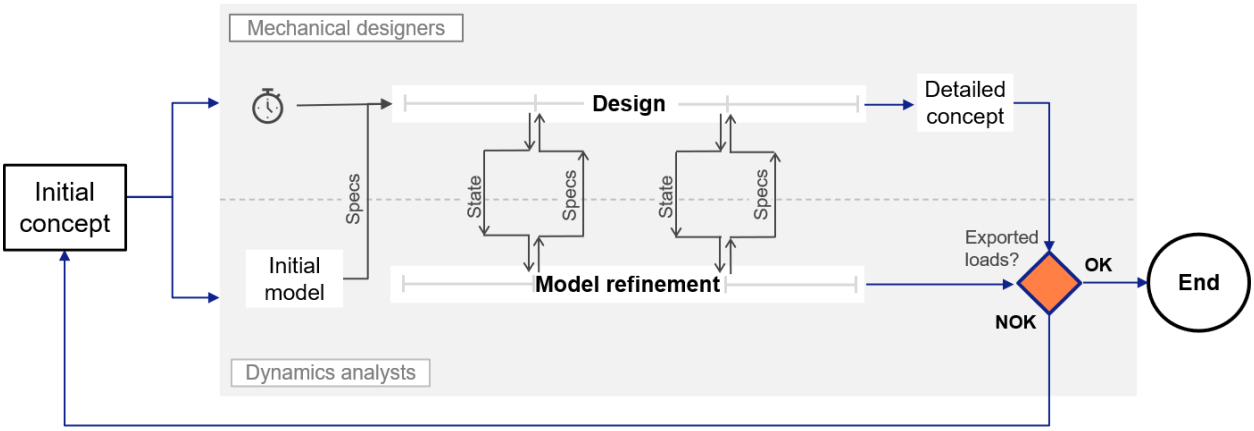

Figure 7. Complete design flowchart showing the position of the project.

In this case, the beginning of the process is almost the same. There is the same initial concept with the top level specification entering the gray box. However, the process is now started by the dynamic analysts, who will develop a rough model of the initial concept to break down the top level specifications into valuable inputs for the mechanical designers. In the meantime, the mechanical designers have not yet entered the project. However, if the initial model takes too long, they will

start the mechanical design without detailed specifications and then again the previously explained workflow will occur (Figure 6). If it goes well the mechanical design team will start designing with specification provided by the first dynamical model.

Additionally, during the design process there is a continuous feedback between the two teams, in which the mechanical designers provide the dynamic analysts with the state of the design so the latter can update and keep refining the model to give more detailed specifications. In this way, the chances of reaching a detailed concept that fulfills the specifications are much higher than before.

One of the objectives of this graduation project is to construct a tool that can help guiding the design of the system in an early stage of the product development. This tool will be located in the "initial model" stage of Figure 7 and will also allow to test different concepts so that it can also be used by system engineers to better determine the starting concept.

2.1. Approach

In order to define this workflow in a more general way, a research on design approaches has been conducted.

A lot of different representations for a V-model exist, some of them are specific for different types of projects depending on the industry and application. A summary of some of the most used V model for these types of applications can be found in (Graessler, Hentze, & Bruckmann). From this, the most appropriate for this specific system is the one by (Eigner, Gilz, & Zafirov) represented in Figure 8.

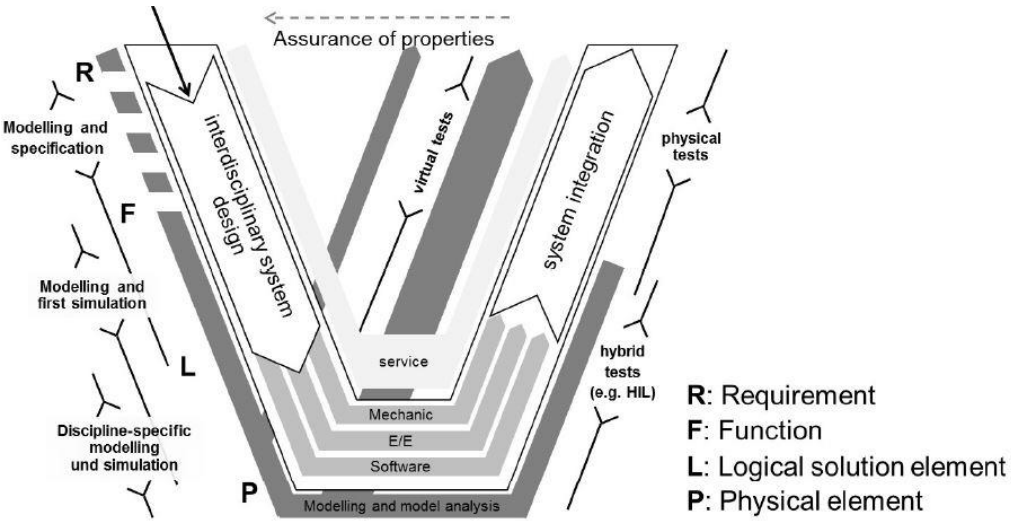

Figure 8. Model based approach V model by Eigner et al. 2012.

The main difference with other methods is that this one clearly defines a position for the modelling phase during the different stages of a project. The approach collects these phases in the so called Interdisciplinary system design. The interdisciplinary system design involves three main stages, R (requirements), F (Function) and L (Logical solution element).

In the first stage (requirement), the customer needs are translated into logically consistent technical requirements. In the second stage (function), breakdown and mapping into functions and

subfunctions takes place. Finally, in the third stage, the solution concept is described by the definition of logical components. As seen in the outer part of the V in Figure 8, the modelling part is represented. The part of interest for the project is the Modelling and first simulation which is located between the second and third stages just described. Mostly quantitative simulation models, e.g. multi-physical simulation models that include several disciplines are created at this stage.

This model-based approach clearly represents what has been explained before with the design workflow between two disciplines. The conclusion is that a model-based approach could have helped to reach a detailed design phase in which the exported reactions specification has been taken into account for the mechanical design and thus the top level specification has more chances of being fulfilled. The main objective of the graduation project is to prove that a model-based approach can break down a top level specification into valuable design parameters to drive the detailed design of the system.

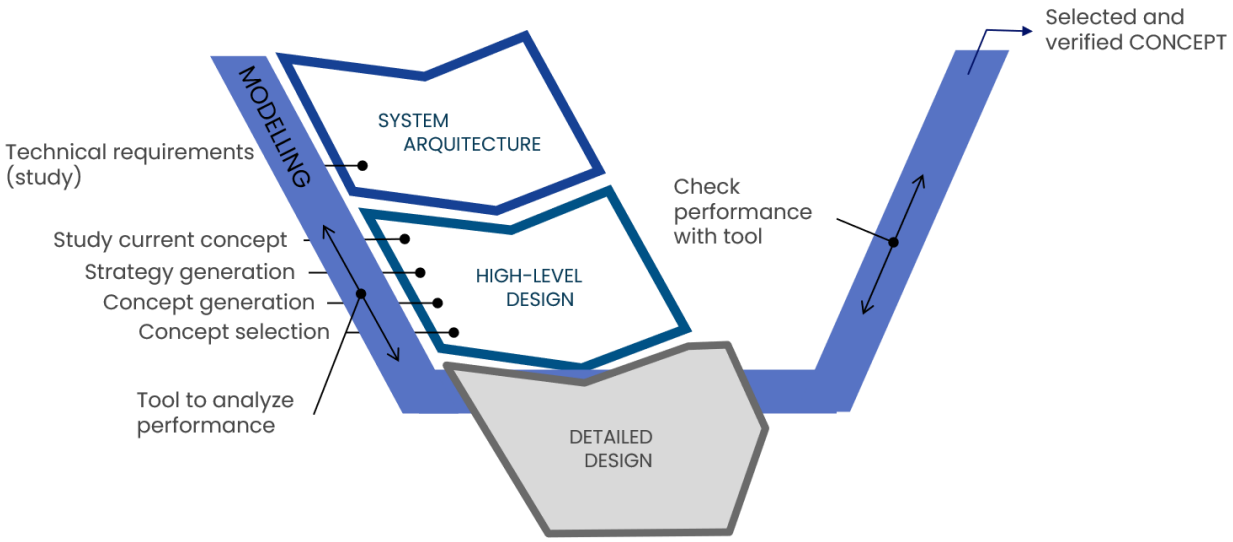

Figure 9. Project V model.

In Figure 9, a close-up of what will be the desired V model representation of this graduation project is shown. The project starts with the study of the technical requirements. The next step is to study and analyze the current design in order to find disturbances to apply in the following stages. As it can be seen in the representation, the planning of the graduation project was to generate strategies and new concepts and analyze those concepts with the development of a model. However, at the end, the graduation project has stayed in the "*Study of the current concept*" and the "*development of the tool* " because of time limitations. However, this representation shows how the future work on this topic should continue. In Chapter 7, a better explanation of the future work with respect to this V-model will be presented.

3. System analysis

In this section the REMA module will be described to give the reader more insight into the current design. First, the functional requirements and the most relevant specifications for this project will be explained. After that, the current physical system and an overview of its components will be presented. The following subsection will go more in depth into the kinematics of two systems of the module, the balance mass and movers. This chapter is entirely rewritten in the confidential annex. For a complete description of the system, this chapter can be ignored and replaced by the confidential Chapter 9.

3.1. REMA System and specifications.

Although the functional requirements have already been roughly introduced in 1.2, they are presented again in this subsection for a better understanding. The functional requirements are:

- The REMA end effectors must block the light in such a way that only areas of interest within the mask are exposed.
- The REMA end effectors must act as a shutter at the start and end of a scan.
- The REMA module must provide a stable and accurate mechanical interface.

As mentioned, one of the functionalities of the REMA is to block the light from impacting non-desired areas of the mask. This is done in two axes, X and Y. REMA can be classified into two big systems: the one responsible of masking the reticle in the X direction and the one responsible for the Y direction. The Y direction is the scanning direction. The X end effectors, which are responsible for blocking light along the width of the exposure slit, are out of scope for this project. During operation they remain almost stationary except for certain actions, which have no influence on the objective of this project.

The focus from now on is going to be on the Y masking mechanism, this system can be decomposed into four big parts: the end effectors, the actuation, the guiding and the balancing system. A description of these parts is presented now.

The first and most important component of the REMA are the **end effectors**, this is the part of the system that blocks the light before it reaches the reticle. The end effectors have to perform the scanning sequence. They are divided into Y1 and Y0, this nomenclature will be used throughout the entire document.

Continuing with the parts of the REMA, the next part is the **actuation system**, which is composed of two main actuators. The Y1 end effector is actuated by one of those actuators in parallel and Y0 by the remaining one. The **guiding system** that connects the actuators with the end effector, is composed of two cylindrical joints per actuator. A more detailed analysis will be shown later on in this chapter.

At last, the **balancing system (or balance mass),** it is responsible for counteracting the reaction forces in Y direction, generated by the moving end effector. The balance mass working principle is to accelerate a mass in the opposite direction of the end effector and guiding system in such a way that the reactions of each of the masses are opposite and thus cancelled (more in depth explanation will be given in the following subsection).

The first and most important specification for the design of REMA is the motion of the end effector, known as setpoints. The REMA end effectors must be driven by specific motion, velocity and acceleration profiles. Even though thousands of these profiles exist, each for a different application, all of them follow a similar trend as the one presented in chapter 9 (confidential).

Continuing with the specifications, the second most important for the design of the system is the so called exported reactions specification. This specification comes from the fact that the REMA module is connected to the same frame as other limiting modules, as the reticle stage, and thus the disturbances that the REMA module can exert to this frame (Top frame) have to be limited. This specification is defined in frequency ranges at the point of interest (PoI) which will be presented in the modelling section.

Having explained the most important specifications of the REMA module, a closer explanation of some of its components will be given in the following subsections.

3.2. Balancing system.

The REMA module is constantly subjected to a variable force that is driving the end effector at every moment. During the working process of the REMA, inertia forces and inertia torques are generated, which are exerted to the top frame as reaction forces and moments. These reactions will probably cause vibrations, which could induce noise, wear fatigue and other position inaccuracies. Therefore, vibrations are a phenomena that has to be avoided. Usually vibration suppression mechanisms are used to tackle this problem, like for example damping or others. However, with this solution the problem is not solved from its root, that is the inertia forces and torques generated by the mechanism. The balancing of mechanisms is the principle that tries to reduce or eliminate these inertia forces and torques and thus, vibrations, from the root of the problem.

In balancing techniques, the sum of the inertia forces that act on the base of the mechanism, are called shaking forces. Next to this, the sum of inertia torques are called the shaking moments. The balancing of a mechanism can be classified in two big groups, static and dynamic balancing. The former makes reference to a mechanism in which just the shaking forces are eliminated or balanced. The latter is used when both the shaking force and moment need to be eliminated or reduced.

Research on balancing has been done for decades and many principles and methods have been described in literature. The most basic idea and frequently used approach results from the conservation of linear momentum law and angular momentum law (Zhang & Wei). This method states the following: the shaking force and the shaking moment of a mechanism will be eliminated if the linear momentum p and the angular momentum h remain constant for any motion at all times. In an equation form will look like:

$$p = \sum_{i=1}^{n} m_i \dot{r}_i = const$$

$$h = \sum_{i=1}^{n} (I_i \dot{\varphi}_i + r_i \times m_i \dot{r}_i) = const$$

with i being the number of the link of the mechanism, m_i the mass of the link, r_i the position vector of its center of mass, I_i the moment of inertia, and φ_i the angle of rotation. These two

constraints are necessary and sufficient conditions for a reactionless mechanism. As a conclusion, from these equations it can be stated that for a force balanced mechanism, its center of mass should describe a constant velocity motion or be stationary.

It may seem that balancing mechanisms only have advantages, but there are also several drawbacks: the addition of mass and inertia to the system, the influence on the input forces or torques needed to drive the mechanism, or the modifications of the machine itself. The addition of mass and inertia and the volume needed to implement the balancing principles are two of the biggest drawbacks. Several techniques and studies like (van der Wijk, Herder, & Demeulenaere) and (van der Wijk & Herder) already demonstrated the possibilities and concluded which methods are the best to reduce these drawbacks.

This brief introduction to balancing mechanisms can give the reader an idea of what is the function of the balance mass system in the REMA module. Now the REMA balance mass will be seen in detail to understand its functionality.

In the REMA module, the actuators are exerting the force to move the end effector. The inertia forces and torques generated by the movement of the end effector are generating the resultant reaction forces to the frame. To reduce this effect the actuation system is suspended in such a way that when the end effectors are actuated, the balance mass itself is actuated in the opposite direction. In Figure 10, the motion of the BM and the end effector can be observed. Three positions are represented: the neutral position and the two limit positions. When the end effectors are completely extended, the BM is in its most backward position and when the end effectors are retracted, the BM is in its most forward position. The arrow in Figure 10, represents the actuation force between the movers and the BM. The joints between bodies and the BM suspension are going to be explained during this section.

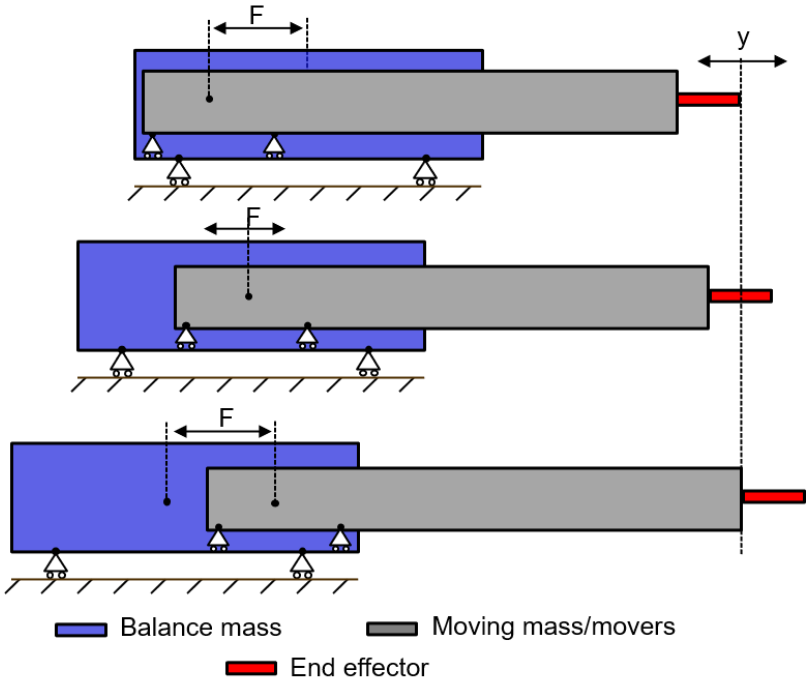

Figure 10. Motion of the BM and the movers.

3.2.1. BM guiding system kinematics.

In this subsection, the kinematics of the balance mass guiding system is going to be explained. The desired kinematics are of the BM guiding system is 1DOF in the Y direction (represented by the green line). To reach that DOF the guising system consists of five 1 constraint joints located in specific constraints planes is such a way that the permissible translation remains in the Y direction. To reach this configuration, the FACT method is used.

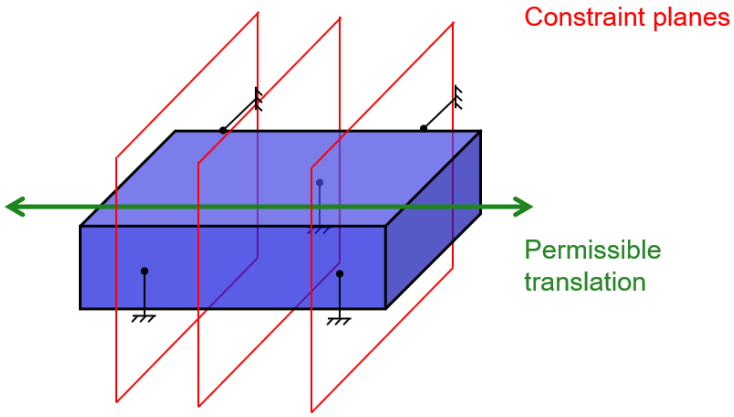

Figure 11. BM guiding system kinematics.

Following this rule, this mechanism is exactly constrained. Over-constraining the mechanism can induce negative effects in the guiding system such as assembly loads and misalignments. A trade-off between symmetric and exactly constrained mechanism has been made. In this case, the two are not possible in the same design or too complicated. However, in this specific system the fact of having a non-symmetric guiding system could also have negative effects on the performance of the mechanism. To continue with this reasoning it is necessary to introduce some definitions.

3.2.1.1. Center of Force, Center of Stiffness and Center of Gravity.

Having explained the kinematics of the current guiding system it is important to have the following definition in mind as it will be used during the analysis of the mechanism.

As explained in (Soemers) the main message of this section is to understand that in a mechanism where dynamic forces are predominant, the best configuration to avoid parasitic disturbances is to place the force application point (or center of force) exactly at the same location as the center of gravity and the center of stiffness (or center of compliance).

To explain this, the same example used in (Soemers) is used. Later in the document, the disturbances on the system will be explained by making use of this concept. Having a single body in a flexure parallel guiding (as in Figure 12a) which is desired to have a pure horizontal translation. The question is where to apply the force in such way that the resultant displacement is free of rotations, no matter which driving force is applied.

Two types of loads are considered: static and dynamic. For a static load, the condition of zero rotation can be imposed by making use of the stiffness matrix for a sheet flexure with perpendicular load. A solution for the force point of application is found. It states that the force has to be applied at half the flexure length in order for the clamping forces and moments of the flexure to not generate any rotations. This means that if the force is applied at point 1 in Figure 12a, the system will

experience a parasitic displacement. It is just when the force is applied at point 2 (or along a horizontal line crossing 2) that the resultant displacement is pure.

That point previously found, is said to be the center of compliance. It can be defined as the point in which a load applied in a certain direction generates a displacement in the very same direction of the load, without any parasitic displacements or rotations.

However, when the load is dynamic instead of static, there is an additional force term. Inertia forces and moments will take part in the problem. If these inertia forces were generated at the center of compliance there would still be no parasitic displacement. However, inertia forces and torques are generated in the center of gravity of the body, which is not at the same location of the center of compliance (as seen in Figure 12c). Then the resultant load is no longer at the center of compliance and thus a parasitic displacement will be generated. From this definition it holds that for a free of parasitic displacements guiding system, the force, no matter at which frequency, should point through both the center of Gravity and the center of compliance. This means that the center of gravity must coincide with the center of compliance or be in line with it, depending on the application and the load direction.

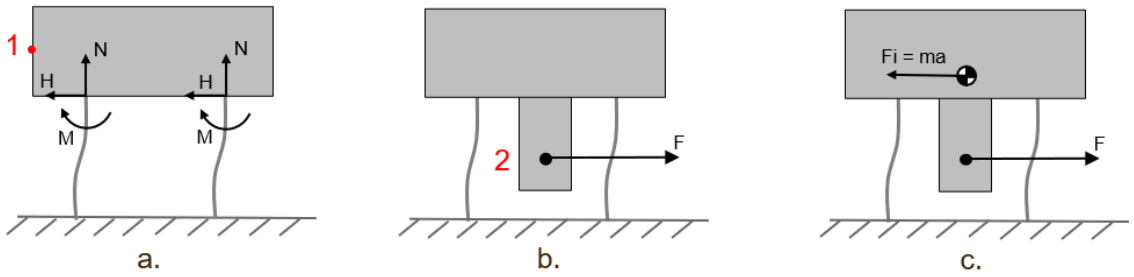

Figure 12. Center of force, Center of gravity and Center of stiffness relationship.

Going back to the balance mass guiding system, the fact that the flexure mechanism is not symmetric means that the center of compliance cannot be intuitively located. Combining this fact with the dynamic nature of the excitation force in the system, it can be concluded that there will be a parasitic displacement generated by the uncertainty in the position of the center of compliance with respect to the center of force and center of gravity of the guiding mechanism. This phenomena is not going to be studied in the project but it is important for further analysis. In fact, this is one of the main simplifications taken during the modelling of the balance mass suspension. The BM suspension guiding system is modelled by four symmetrically distributed constrains with a stiffness equivalent to the stiffness of the exactly constrained configuration. More in depth explanation of this assumption is done in chapter 9 (confidential).

3.3. End effector guiding system

In this section the kinematics of the end effector guiding system will be analyzed. The objective is to understand the function of every component in the kinematics of the subsystem in order to model it correctly.

The desired kinematics for this system is to have a 1DOF translation along the Y axis for each end effector, Y1 and Y0. Two DOF translational in total. The analysis will be done just for the Y0 end effector and it is also applicable for the Y1.

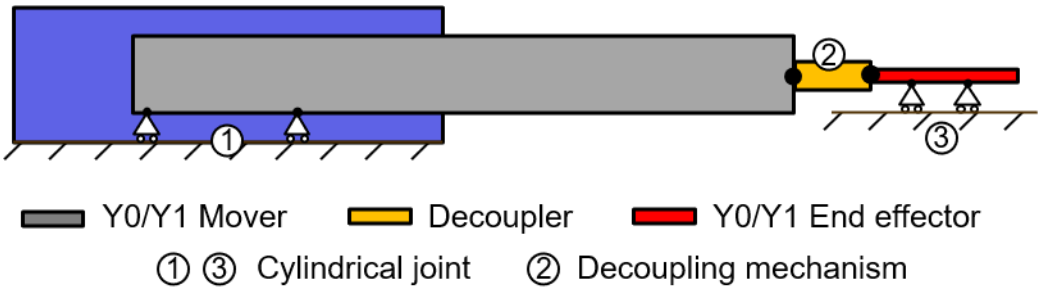

Figure 13. Schematic of the end effector' guiding mechanism,

In the case of Y0 subsystem, there are three bodies (mover, decoupler and end effector) in reality there are much more components inside every of these parts but the connections between those components are rigid an thus are not considered for the DOF analysis. The joints present in the mechanisms are the following:

- Cylindrical joint (CJ): restricts 4 DOF. Permits the translation and rotation along the shaft axis and constrains all translations and rotations orthogonal to the shaft axis.
- Decoupling mechanism hinge: restricts 4 DOF per hinge. Constrains two translation and two rotations.

Knowing the main properties of the joints, a DOF analysis can be performed. By subtracting constraints to the total DOF of the three bodies. A total of 2 DOF remain.

$$6\,(DOF)\cdot 3\,(bodies)-\left(4\cdot 2\,(CJ)+4\cdot 2\,(hinge)\right)=2\,DOF$$

The remaining 2 DOF are the translation and rotation along the Y axis. Although it is not represented in Figure 13, an additional mechanism to limit this rotation exists in the mechanism. This mechanism is not included and a simplification is done to limit the rotation in Y. This simplification is explained in Chapter 4.

In this subsection, the kinematics of both Y1 and Y0 subsystems have been explained. It can be concluded that both subsystems have 1 translational degree of freedom along the Y direction. Having explained the kinematics of both the balance mass and the guiding system of the end effector, the next subsection will be focused on the disturbances that have been identified in the system.

3.4. Parasitic disturbances

In this section, the possible parasitic disturbances identified in the system will be explained. Some of them are explained in this subsection but not analyzed in the analysis chapter. However, it is important to take them into account for the modeling section and conclusions. Before listing the disturbances, the points through which the loads are transferred to the REMA frame are presented. In Figure 14, the different loads paths can be seen.

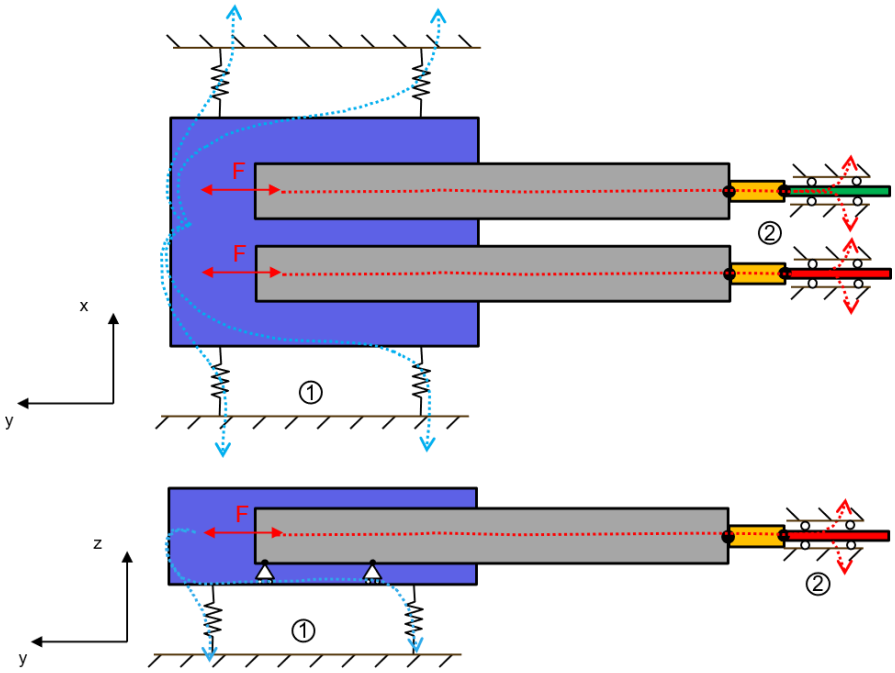

Figure 14. Representation of the different load paths in the mechanism.

There two load transmission points from the mechanism to the REMA frame. The blue path corresponds to the forces transferred through the BM guiding mechanism and it consists of 4 points (number 1). Next to this, the red path represents the transfer of loads through the front cylindrical joints (number 2).

The identification of the disturbances has been done by use of the relation between COG, COF and COS.

1. **Actuators positioning**: this disturbance makes reference to the manufacturing and assembly errors that affect the force line one of action. As represented in Figure 15, the two situations shown, result in the line force of action not being in line with the Center of Stiffness (COS) and the Center of Gravity (COG). This misalignment will generate a force component in the a non-balanced direction that will directly be transferred to the frame.

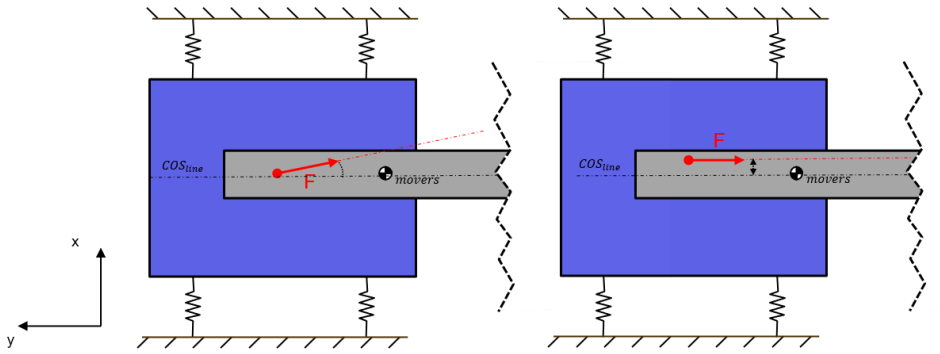

Figure 15. Disturbance due to actuators inaccuracies.

2. **Non-linearity of flexure guiding system**: The guiding mechanism of the balance is composed by elastic elements. These elastic elements have a nonlinear stiffness in its stiff direction. The support stiffness of the mechanism varies along the stroke. When the balance mass is moving in Y direction, the stiffness of the BM guiding mechanism in Z direction is constantly changing. Apart from the nominal Z displacement of the BM due to static gravity loading, an additional drop in Z direction is expected due to this loss in support stiffness. In Figure 16, this disturbance is represented. This will affect the system in several ways that will be seen in the analysis chapter. The functional stroke of the balance mass is below 10mm, this results in a loss of support stiffness up to 25% of the stiffness in the zero stroke position.

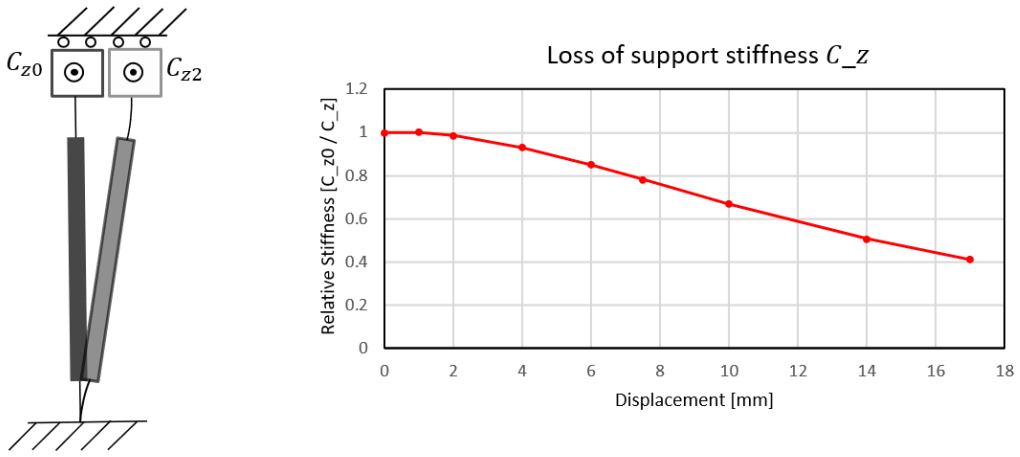

Figure 16. Example of the loss of support stiffness in a flexure mechanism.

3. **Misalignments in flexure guiding**: positioning misalignments in the assembly of the flexures that suspend the balance mass could introduce stresses in the flexures which will lead to unknown disturbances into the system. Disturbance affecting the location of the Center of Stiffness (COS).

4. **Distribution of gravity loads**: The position of the various COG in the mechanism along the Y axis is constantly changing due to the motion of the mechanism. The main driving force

is acting in the Y axis. As long as the Z position of the COG remain constant and in line with the COS, no disturbance will be created due to this relative position.

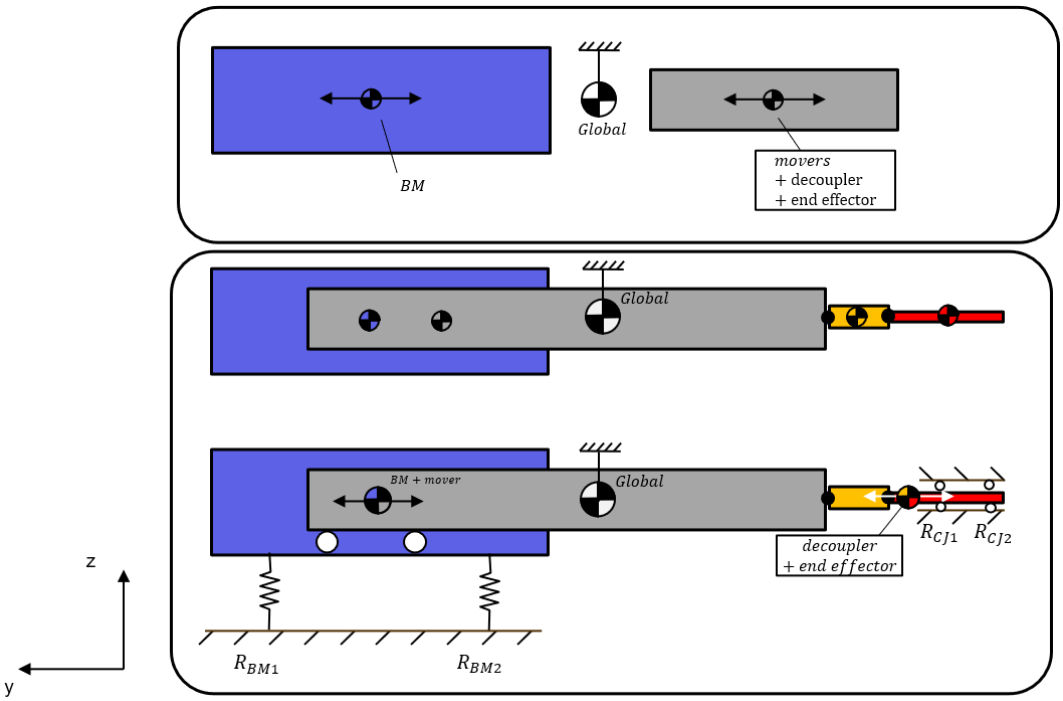

Figure 17. Representation of COG motion.

On the other hand, the gravity load is always in line with the COG but not necessarily with the COS. In section 3.2 the dynamic balancing concept was explained. From that explanation it was concluded that the global COG of the whole mechanism will remain stationary in every moment if a BM is included. In Figure 17, the motion of the COG in the YZ plane is represented. The BM is designed to counteract the accelerations generated by the combination of mass of the mover, decoupler and end effector. If the bodies are grouped depending on where the gravity loads are being transmitted, the representation is as in the bottom sketch in Figure 17.

On one side, the BM plus the mover and on the other side, the decoupler plus the end effector. Maintaining the condition that the global COG remains stationary, it can be said that both combined COG are experiencing a motion. For the combination of decoupler and end effector it is straightforward as both bodies are moving together in the same direction at every moment. This means that the Z gravity load in the front cylindrical joint ($R_{CJ1} + R_{CJ2}$) is constant along the stroke, as it is always supporting the same weight combination. However, the Z reaction forces and moments in each of the contact points R_{CJ1} or R_{CJ2} will be constantly changing along the stroke, due to the motion of the COG.

On the other hand in the BM connections it is less intuitive because each body is moving in one direction, when the movers moves to the front, the BM to the back. However, as the BM displacement is obtained by a ratio of the combination of movers, decoupler and end effector, if it is combined just with the mover, this combined COG will experience a displacement. Thus, the total Z reaction load ($R_{BM1} + R_{BM2}$) is constant along the stroke

(always the mass of the BM combined with the mass of the movers). However, locally, each flexure will have a varying Z reaction and moment. The fact that the total Z load in each connection point is constant is due to the decoupler, which does not transfer any mass in Z from the balance mass and movers to the end effector.

4. Modelling.

This chapter describes the multi-body model of the ReMa module developed during the project and used for the analysis and conclusions. The objective of the model is to analyze different disturbances for the exported reactions of the whole REMA module and to find and describe smaller specifications for the involved disciplines. The assumptions and simplifications taken during the modeling phase will be described during the chapter. It is important to remark that this model is based on a current, already designed, REMA module. However, it has been abstracted to an early development phase to fit the main objective of the project. Some of the readers may have more knowledge about this system and may find some of the simplifications or assumptions not a good representation of reality. Bear in mind that this model is not trying to represent the current system but to anticipate possible problems that could appear in a detailed design phase by tackling them in an early development phase.

4.1. Description of the model.

A multi-body model allows the designer to analyze all the reactions generated by the motion of rigid or flexible bodies connected with kinematic joints. The focus of the model are the reaction between the REMA module and the force frame of the machine. The disciplines involved in this analysis are mechanics and dynamics, being also possible to add more modules and disciplines to the model. The software used is MATLAB Simscape multibody (Simscape, 2021). A selection between different software was made, being this the selected one mainly due to the facility to build the model and the possibility of integration of more disciplines like control, electronics, fluid dynamics…

To start with some assumptions, the most relevant is the consideration of rigid bodies, despite the fact that the Software allows to model flexible bodies this assumptions makes sense if you think that in an early stage, the geometry of the bodies is not defined and thus nor its stiffness.

The input in the model is the motion profile of the end effector, thus the actuators force generated between the moving masses and its support. The detailed description of the input can be found in the confidential chapter 9.

The model consists, of 11 bodies. All solid properties have been exported from the CAD model except from the geometry, which have been simplified for modeling purposes. At the end, all the bodies have the same mass and inertia properties as in the CAD. During the analysis, some of those properties will become design/analysis variables. An overview of the solid bodies and kinematic joints can be found in Figure 48 (confidential) or in the summary section.

In order to define the joints between bodies, the desired kinematics of the mechanism analyzed in section 3.2 and 3.3 have been applied. The degrees of freedom per joint have been defined and different types of joints have been selected. In Figure 18, a representation of all joint connections per body and the type of joint can be seen. For the mover, end effector and decoupler, just the Y0 mechanism has been represented, the same holds for Y1. Next to this, a description of every joint type is presented.

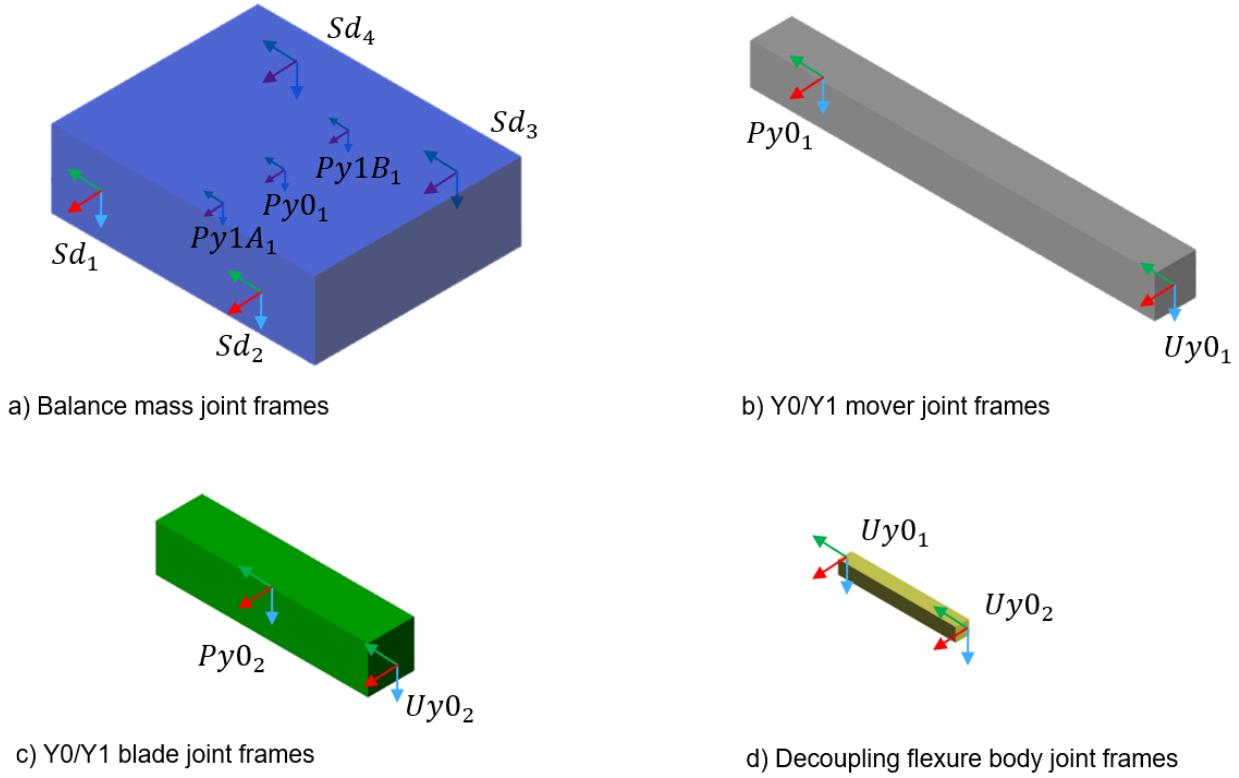

Figure 18 Joint location and type of kinematic joint for the simplified solids.

Rema frame to Top Frame joint (PoI): this connection is a rigid connection between the REMA frame and the Top Frame and it defines the point where the global reactions are analyzed, the Point of Interest (PoI). In reality this connection has a stiffness and damping as all mechanical systems. However, as a simplification this stiffness has not been included in the model.

Balance mass to REMA frame joint ($\boldsymbol{Sd_1 - Sd_4}$): one translational degree of freedom in Y direction is desired for this joint. The objective of the balance mass is to counter act the accelerations generated by the moving mass. The balance mass needs to have a free movement in the Y direction. The joint chosen to allow this, is a 6 DOF joint. This joint allows to set stiffnesses and damping in all directions (X, Y,Z, rotation). The mechanism that is guiding the balance mass, is a compliant mechanism. Such mechanism has theoretically one DOF. However, its stiffness is not infinite in all the other directions, thus it is crucial to include these stiffnesses in the model in order to include possible misalignments and disturbances in the constraint directions. An example of this disturbances is the loss of support stiffness introduced in section 3.4.

Y0 mover/Y1 mover to BM joint ($\boldsymbol{Py1A_1, Py0_1, Py1B_1}$): This joint is where the actuators are exerting the force to drive the moving mass and the balance mass. In the real system this joint is a cylindrical joint. This joint has zero stiffness in the free direction and a specific stiffness and damping in the radial direction. The effects on this joint are out of scope for the project so, to avoid the need of an extra joint to limit the Y rotation (that was left free as analyzed in the kinematics section 3.3) it is modeled by a prismatic joint with infinite stiffness in the radial direction.

Mover to end effector joint ($\boldsymbol{Uy0_1, Uy0_2}$): the objective if this joint is to decouple the mover from the end effector in such a way that misalignments on the balance mass system does not affect the end effector positioning. This joint generally constrains the relative displacement in Y direction and Y rotation between the movers and the end effector. To model this joint, a rigid body between the

mover and the end effector has been added. This body is connected in one side to the mover with a universal joint and to the end effector in the other side with the same joint type.

End effector to REMA frame joint (Pr2): The end effector is guided by a cylindrical joint closer to the point of accuracy. To model this joint, the same approach as in the movers to balance mass joint has been used, a prismatic joint. This is a simplification and it has the drawback that the radial stiffness and damping are not included in the analysis.

In Figure 19, a graphical representation of the three types of joint used in the model is presented. In each free Degree of Freedom, stiffness and damping can be added.

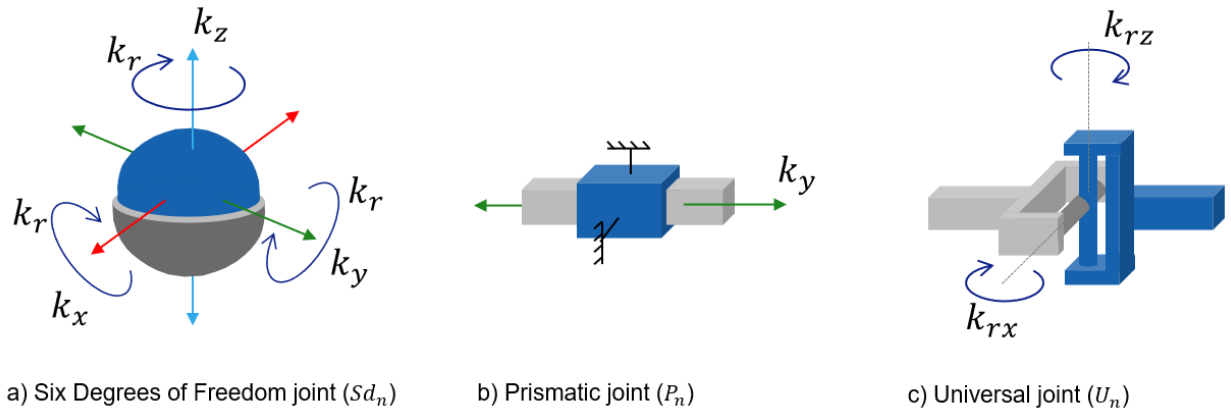

Figure 19. graphical representation of the types of joints used in the model.

For the assembly of the bodies, the relative position have been exported from the CAD. The final assembly of the bodies in the model is presented in Figure 20 (see Figure 49 for the confidential version of the figure).

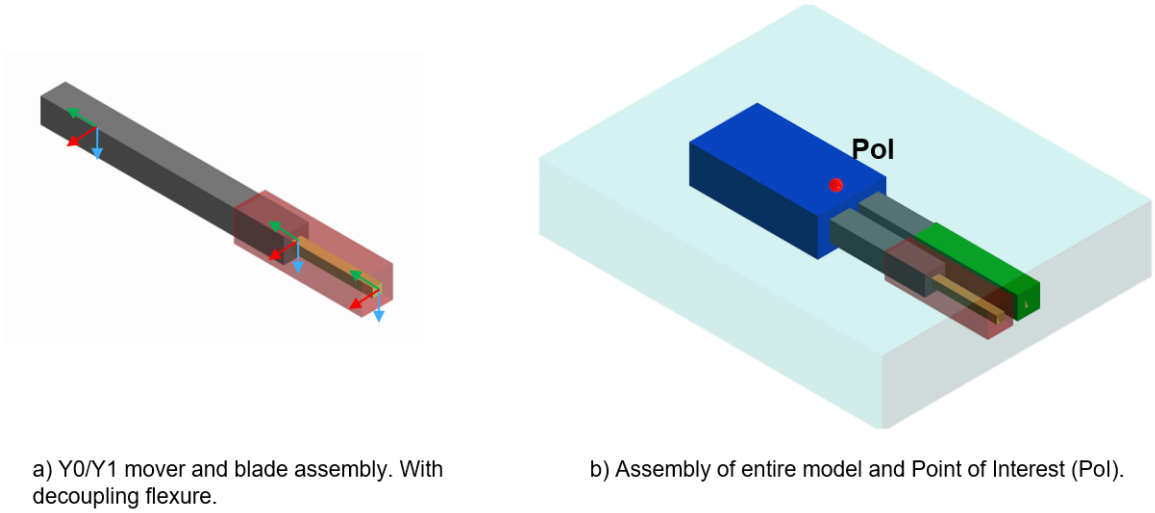

Figure 20. Model assembly.

Until this point, the bodies, connections and assembly of the model have been presented. In the following subsection the inputs and output possibilities from the model will be explained.

4.2. Model variables/parameters.

In this subsection the input parameters and possible outputs from the model will be explained. A layout view of the model in MATLAB Simscape Software can be found in 10.

The inputs to the model all come from the current design (CAD) and from specifications. With respect to the output from the model, the main interest is the reaction forces. The reaction forces and torques can be measured in several ways:

1. In a joint: every joint allows to measure the reaction forces generated inside that specific joint in every direction, even if in that specific direction there is rigid constrain. For example, in a prismatic joint in which the free direction is lying on the horizontal plane, (and the vertical plane is gravity direction) the reaction forces due to gravity can be measured.

2. Between two frames: at every part of the system, even if there is not a joint, a force measurement sensor can be placed to analyze the reactions.

Other valuable outputs for the analysis of the system are the position, velocity and acceleration of specific points of the mechanism or bodies. For this output there is also the possibility of placing a sensor at every point of the system between two frames. The second option is again measuring at a joint, in this case just the values in the free directions can be analyzed. The same applies for angles, angular velocity and angular acceleration.

In summary, all dynamic parameters can be extracted from the model if there is a frame in the point of interest. For example, if the displacement on the tip of the end effector has to be analyzed, it is necessary to locate a frame in that specific position in order to obtain the necessary data. Thus, it is important to know which is the desired data that is going to be needed from the model in order to avoid several iterations for every measurement.

4.3. Assumptions.

In this subsection, the assumptions made during the modeling phase will be described.

- Rigid bodies: all the bodies are considered rigid. Specific bodies could be upgraded to flexible bodies if the analysis requires it. The software allows this possibility in different ways (Miller, Soares, Van Weddingen, & Wendlandt).

- Actuators' force: the actuators are modeled as a force source without any disturbance/misalignment, they can produce the desired force to follow the motion input without imitations. The force is perfectly centered in the specified point. Errors in the manufacturing/assembly of the actuators that could lead to a misaligned center of force are not considered.

- Products of inertia: Despite the fact that all considered bodies have a non-diagonal inertia matrix, that is, they do not have a symmetric mass distribution along its' general axes. As a simplification for the study and understanding of the results, the products of inertia have been set to 0.

- Cylindrical joints: modeled as prismatic joints in which the radial stiffness and damping cannot be analyzed. It limits the rotation about the Y axis an thus no additional mechanisms is needed to constrain that DOF.

- Stiffness in moving direction of the BM flexures: generally considered to be zero as in an ideal case but will be set to the a specific value for certain analyses (as in Case two in 5.1.)

- COG positions: The COG position of all the bodies has been measured in CAD. However, in the model the COG have been placed in the ideal or desired position. In Figure 21 (see Figure 50 for the confidential version of the figure), the COG and force line of action are represented. Every COG has been positioned to be in line with the COF in the XY plane (represented in Figure 21a & Figure 21b). That is, the Z coordinate of all COG is the same. Next to that, the distribution of the COG is symmetric with respect to the YZ plane (represented in Figure 21c. That means that the COG of both Y1a and Y1b movers have the same X coordinate but opposite signs.

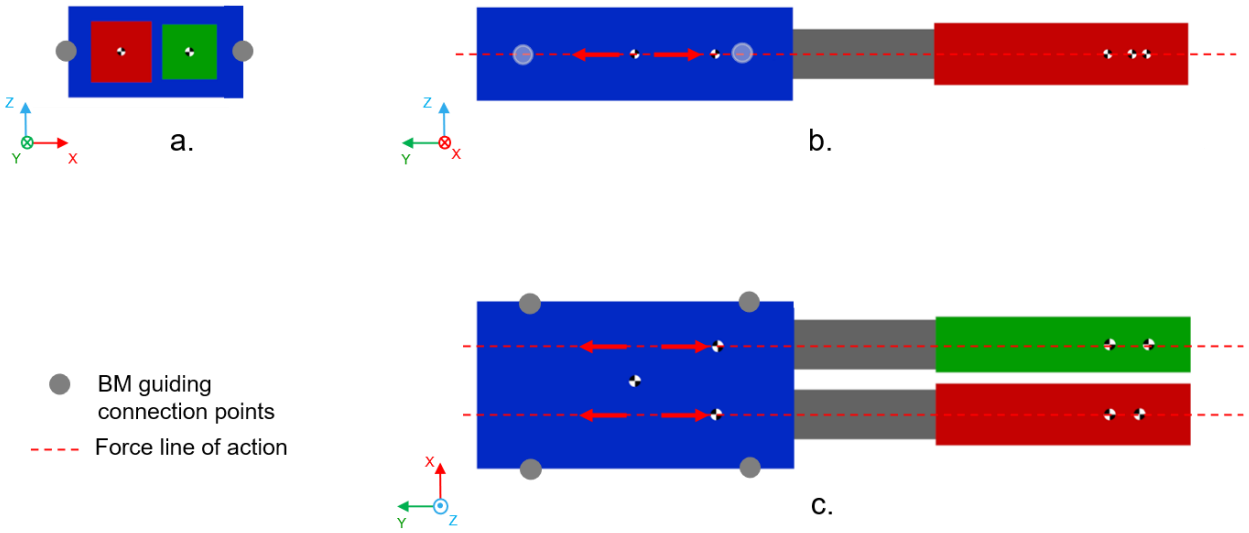

Figure 21. COG, COF and Flexures connection points.

- BM stiffness symmetry: symmetric suspension system with four connection points instead of asymmetric five connection points (connection points as in Figure 21). The distribution of these connection points influences the position of the COS. The symmetric distribution makes the location of the COS intuitive. It is assumed that the position of the connection points for the flexures to the BM is in line with the COF (represented in Figure 21b and Figure 21c).

In this subsection all the assumption made during the modelling phase have been explained. This assumptions are a starting point for the analysis phase and some of them can be eliminated to study specific disturbances of the system. In the case of the COG position and the location of the connection points of the BM flexures, it is known that the current design is not following this assumptions: the distribution of the connection points of the flexures is not symmetric, and it is also not in line with the COF. The reason why this assumptions are made is to be able to eliminate this disturbances of the analysis that are going to be performed. The influence of this parameter is out of scope for this project but it is considered for further analysis.

5. Analysis.

In this chapter, the analysis of different effects on the system will be explained. First, the influence of the balance mass (BM) on the exported forces will be analyzed. Secondly, with a detailed study on the balance mass motion in the YZ plane (specifically), several effects will be found that affect the exported reactions in the BM flexures. The impact that these effects cause on the rest of the guiding system will be shown. To conclude, two solution paths are studied.

It is crucial to remind the reader that the main objective of this analysis is to break down the top level requirement of the exported reactions and motion, into valuable design paraments as an input for the designers. The expected results from this analysis are different, multidisciplinary effects to which a specification could be defined for each of them. All the effects found in this section will have an effect on the exported reactions or in the general performance of the module.

5.1. Analysis of the need of a Balance Mass

To start the analysis section, a general analysis of the need of a Balance mass in the system has been performed. Before starting, the frequency content of the input motion (Figure 22) is presented as a reference for the following analyses.

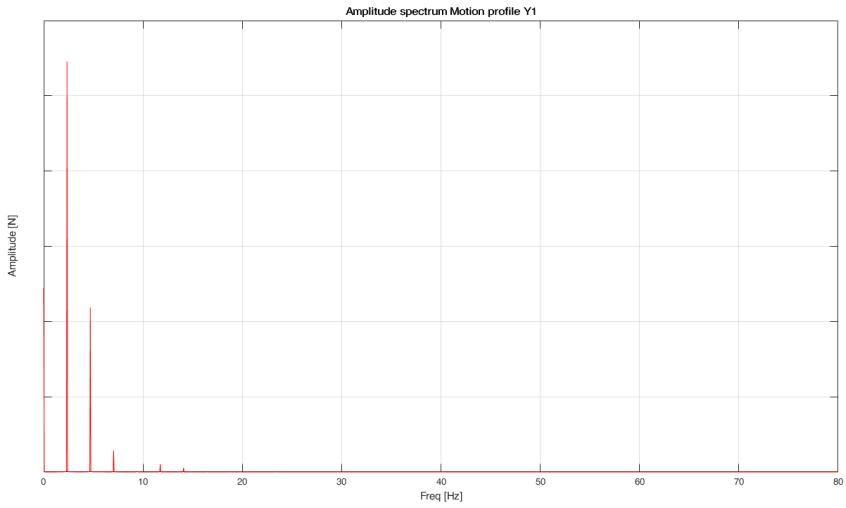

Figure 22. Motion profile amplitude spectrum.

The frequency content of the used motion input for all the analysis is as represented in Figure 22. This is just one motion input of the thousands that exist and thus the results from these analysis cannot be taken as valid for every situation (motion profile). In order to have a clear representation of the exported reactions for all the situation, these analyses should be done for all the motion profiles, as each of them has a different frequency content. It will be seen that the exported reactions results in the frequency domain are dominated by the frequency content of the input.

Three cases are going to be presented in this section, the representation of the cases can be seen in Figure 23. For every case, the reaction forces (in the point of interest (PoI)) in Y and Z as well as the reaction torques in X will be presented, the remaining reactions are not shown because they either not relevant or zero due to assumptions. Case 1 is the analysis of the reactions of the system

without balance mass. In the second case, the balance mass is added. However, the stiffness of the balance mass guiding mechanism in the moving direction (Y) will be set to zero In case number three the stiffness of the balance mass in the moving direction is added.

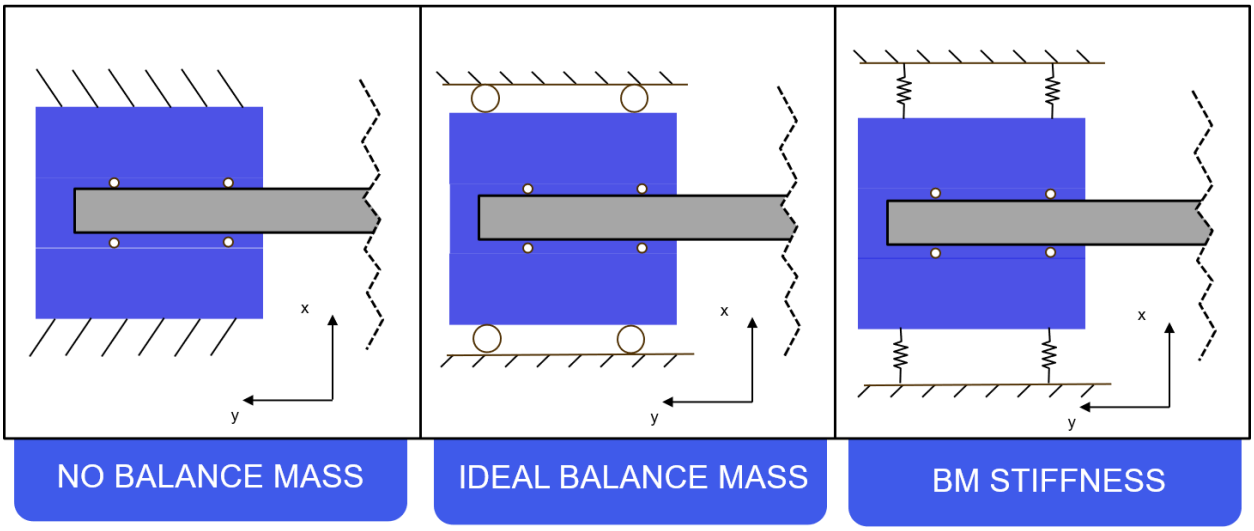

Figure 23. Graphical summary of cases to study in this section.

In Figure 24, both time and frequency domain results are shown. In the right part of the graph, the corresponding amplitude spectrum of each reaction can be seen. The model is considering rigid bodies, no contribution to the high frequency range is expected from these analyses. The reaction forces and moments are calculated in the Point of Interest (PoI) (see Figure 20 to see the location of this point).

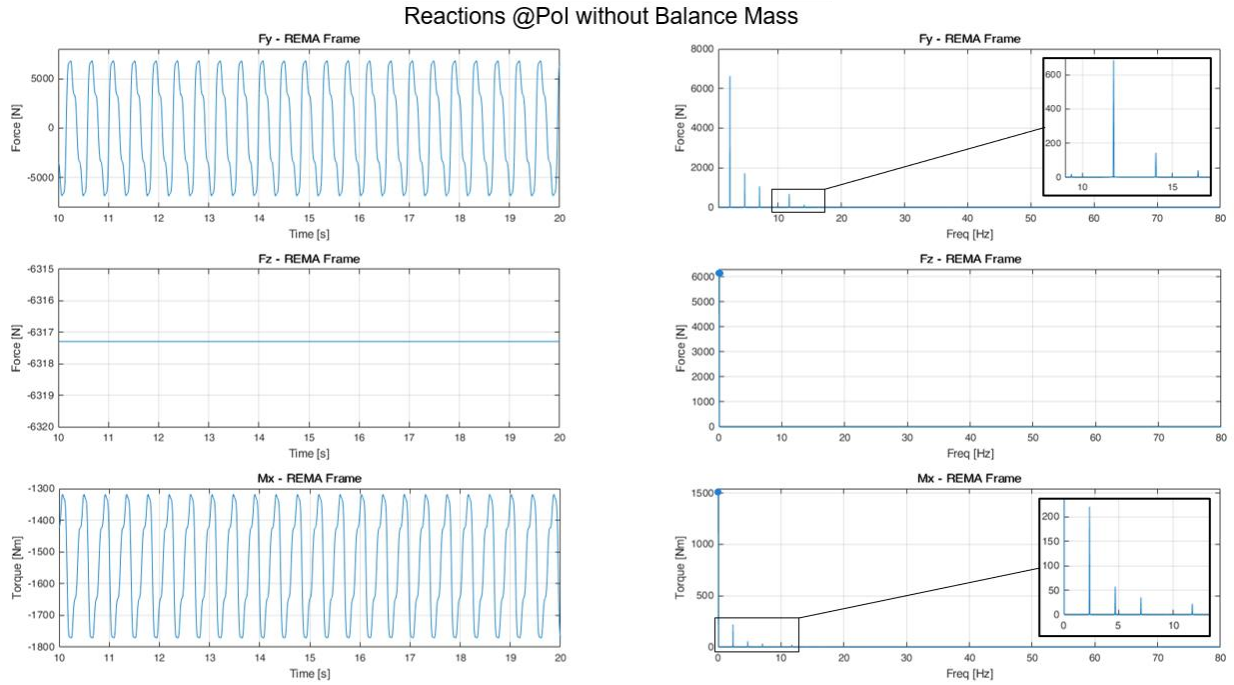

Figure 24. Results from case 1. No BM.

The exported force in Y are quite high due to the high acceleration of the moving mass and the moving mass quantity itself. Moreover, the Y force is not constant but experiences a variation, from the frequency content it can be seen that it matches with the motion profile frequency content. This is due to the fact that no other disturbances are present in this situation. These reaction force is a combination of the mass and acceleration of Y1 and Y0 movers.

The reaction force it Z, on the other hand, it does not experience any variation, no disturbances present in Z direction. The content of this reaction is purely due to mass times gravity and is constant in every moment for this case study.

At last, the moment around X axis does experience a variation and has the same frequency content as the input motion. These reaction torque is present due to the motion of the COG with respect to the Point of interest (PoI) which is fixed to the frame. Remember that in this case study there is no BM and thus the COG position is constantly changing.

Before continuing with the second case (activation of balance mass) a fast calculation to understand the need of a BM is performed. The two most direct solutions to reduce the exported forces are either to reduce the acceleration or to reduce the total moving mass. The acceleration cannot be altered because it is a requirement that directly affects the throughput of the machine. However, the mass is a design parameter that can be imposed. The Y reaction force is $\{F_y = m \cdot a\}$, and the exported force in Y (most critical) has to be lower than 150N for the lowest frequency range. If this limit is to be fulfilled, the total moving mass has to be lower than 500 grams, which is infeasible considering the minimum components that are critically needed in the system. Thus, a system to reduce this shaking force is needed for the exported reactions specification to be fulfilled.

The next step is to introduce the Balance Mass and its guiding mechanism and see the effect it has on the exported reactions. This case 2 has a balance mass whose guiding mechanism is ideal and has no stiffness in the moving direction. In Figure 25, the results for case study 2 can be seen. Again the results are presented in the Point of Interest (PoI)

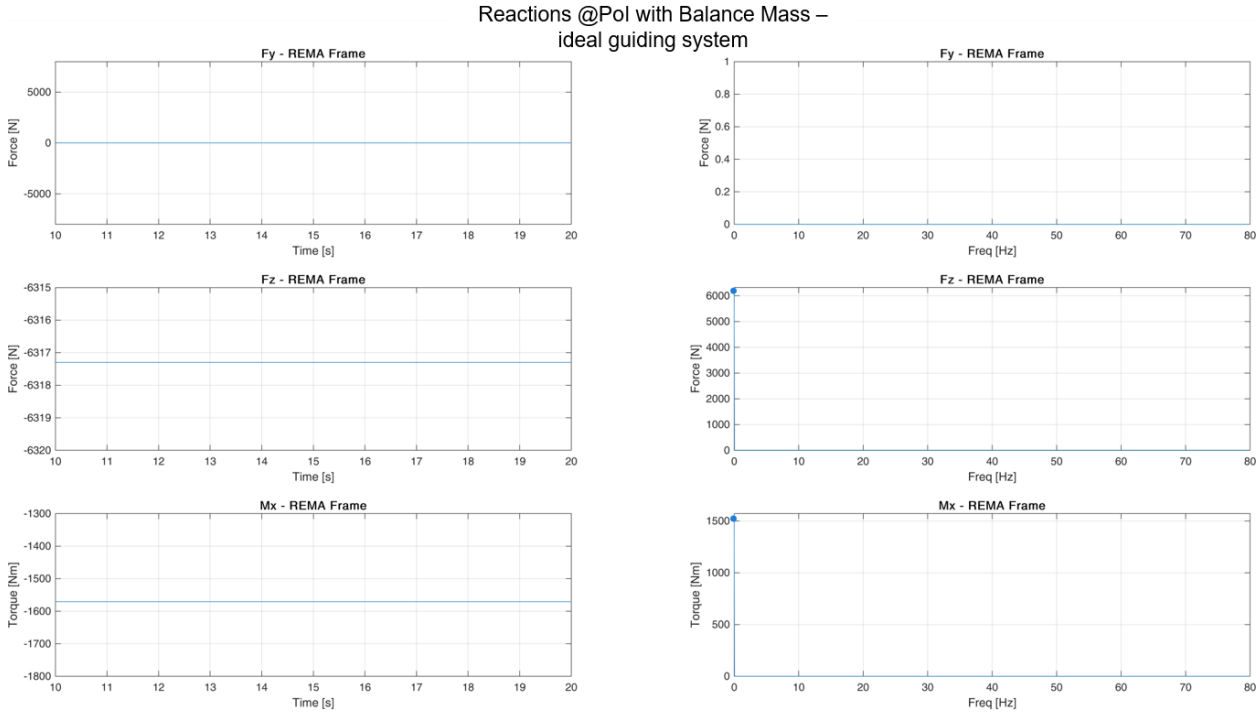

Figure 25. Results from case 2. Ideal BM.

As expected, the reaction force in the moving direction (Y) is completely eliminated as we are dealing with an ideal system which has no other disturbance forces apart from the input force. The Z reaction force remains exactly the same as in case study 1, no changes have been done that affect this reaction. The total mass of the system is the same in this case.

At last, the variation in the moment around the X axis that was happening in case 1 is no longer visible. This is due to the fact that in case 1 the total COG was experiencing a motion. However, in this case (2) the global COG remains stationary at every moment (in plane YZ at least), then the X reaction torque is constant but not zero. It is not zero because the global COG is not in line with the point of interest (PoI)

For the last case, stiffness in the moving direction is added (k_y of the joints Sd_1 *to* Sd_4 , see Figure 18) to the analysis, the results experience a significant change. The result are presented in Figure 26.

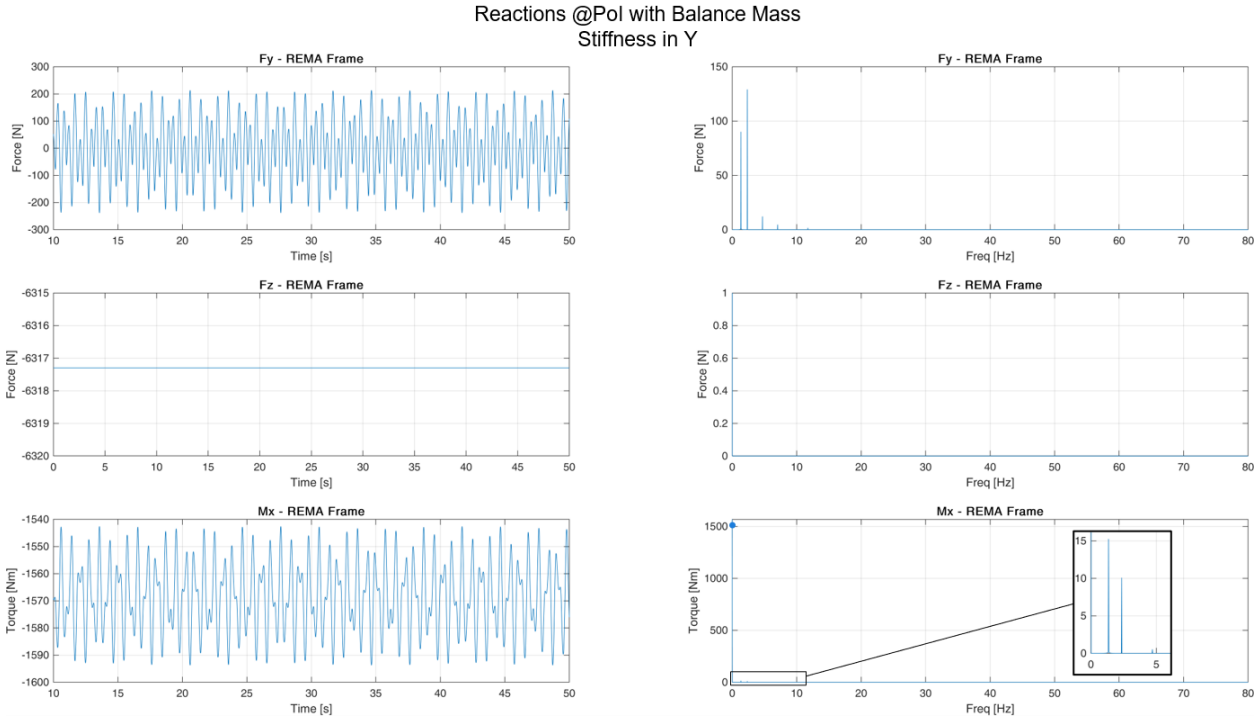

Figure 26. Results from case 3. BM with stiffness.

In the Y reaction force, a new variation has appeared. This is due to the stiffness of the BM guiding mechanism. This stiffness in creating an additional reaction force in the moving direction. The inertia load of the BM is now not the same quantity as the moving mass inertia loads because part of the force is lost in the springs. The part of the force that is stores by the springs is directly transmitted to the frame and is the one that can be seen in the plot.

In the amplitude spectrum of Y reaction force, an extra peak can be seen at a frequency of 1.3 Hz. This peak corresponds to the natural frequency of the balance mass guiding system in Y direction. So now the limiting parameter for the exported reactions is the stiffness of the BM guiding system. This reaction force in Y is directly dependent on the stiffness of the BM guiding mechanism and also on the stroke of the BM. Moreover, the stroke of the BM is dependent on the mass ratio between the moving mass and the BM (around 1/10). If the Y reaction force is to be reduced, several parameters can be changed. The reduction of the stiffness of the BM guiding system, the reduction of the BM stroke and the addition of a separate actuator.

The balance mass guiding mechanism consists of a compliant mechanism which has a limit on the minimum achievable stiffness. By increasing the mass of the BM, its maximum displacement decreases proportionally. However, volume conflicts may arise from a mass increase. A combination of both measures could be a good approach to reduce the guiding mechanism contribution to the exported forces. Additionally, external actuators can be used to eliminate the reaction forces generated by the BM guiding mechanism while at the same time serve as a position control for the BM.

In Figure 27, a free body diagram is presented to explain the function of the BM motors on the Y reaction forces.

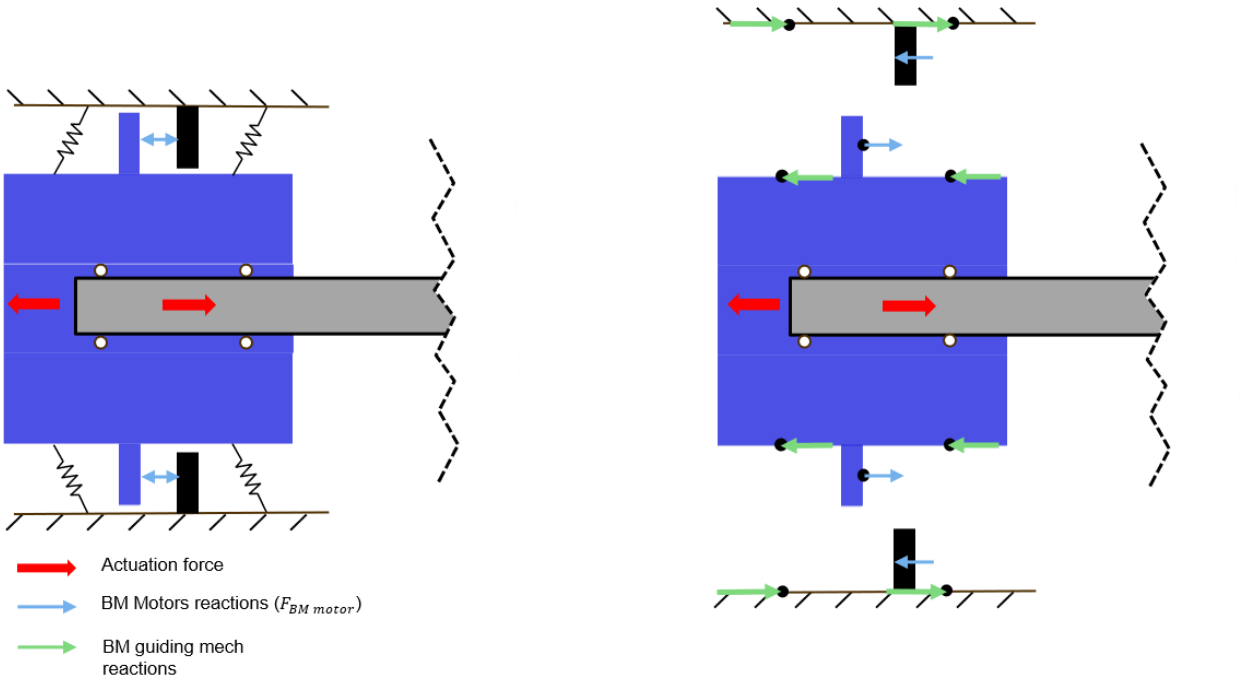

Figure 27. Graphical representation of the function of the BM motors.

These motors act between the frame and the BM and generate the force needed to counteract the Y force of the springs in such a way that a free movement of the BM is ensured.

The Z reaction force remain the same as in the previous cases. However, the moment around the X axis increases due to the same reasons as in the Y reaction force. The global COG is now experiencing a motion and this motion is shown in the X torque variation.

In **Error! Reference source not found.**, an overview of the exported reactions of the three case just studied can be seen.

Table 1.Summary of the results from the 3 cases studied.

	Case 1			Case 2			Case 3		
	Fy [N]	Fz [N]	Mx [Nm]	Fy [N]	Fz [N]	Mx [Nm]	Fy [N]	Fz [N]	Mx [Nm]
Max.	-6824	-6317	-1765	0	-6317	-1545	-226	-6317	-1593
0.1-4 Hz	6646	0	220	0	0	0.03	130	0	15.3
4-9 Hz	1736	0	58	0	0	0	12.2	0	0.53
9-20 Hz	686	0	23	0	0	0	1.6	0	0
20-80 Hz	144	0	1.3	0	0	0	0	0	0

From this analysis it can be concluded that:

1. The mass of the movers needs to be below ~500 grams if no BM is to be added.
2. A balance mass is needed in the system for the exported reactions to be fulfilled in the low frequency range.
3. The BM motors should be able to exert 130N peak force to counteract the BM stiffness contribution to the frame.
4. A trade-off between mass, stroke and stiffness is necessary in the design of the balance mass as it directly affects the exported reactions.

5.2. Balance mass motion analysis.

The effects of the balance mass motion on the exported forces will be analyzed in this section. Two main characteristics that affect the motion of the BM are analyzed. These characteristics are the relative position of the COG of the movers with respect to the COS of the BM guiding mechanism and the variable support stiffness of the BM guiding mechanism. The effect of these disturbances on the exported reactions is then presented.

As explained in the previous section 5.1, the BM guiding system was considered to be ideal in the moving direction (stiffness free). To avoid the influence of other disturbances apart from the ones of interest for this section, the analysis will be performed with the assumption of free of stiffness guiding mechanism in the moving direction.

As it can be seen in Figure 28, there are two points in the system through which the forces can be transmitted to the frame. Those points are the BM flexures and the front cylindrical joints. The exported reactions in those points are the main interest for this section. In section 3.6, a disturbance due to the distribution of the mass over the system was explained. That disturbance is the first that is going to be analyzed in this section.

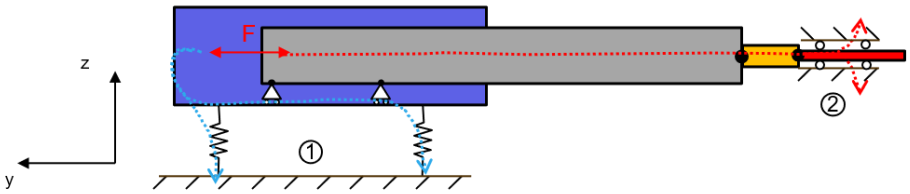

Figure 28. Loads paths to the REMA frame in side view (YZ plane)

In Figure 29, a side view of the mechanism with the combined COG of BM and mover and the COS of the BM guiding mechanism is presented. In the figure, the balance mass is in the neutral position (position zero). The COS of the BM guiding mechanism is located at the same Z coordinate as all the COG in the system (located there on purpose). However, for the ease of the representations it will be located in a lower Z coordinate. In Figure 29b, the combined COG is located. In the neutral position the combined COG is to the right of the COS in Y direction. Having a symmetric guiding mechanism with the same stiffness in all the flexures will result in a bigger displacement in the front flexures and thus, the BM will experience an angle around the X axis (Figure 29c).

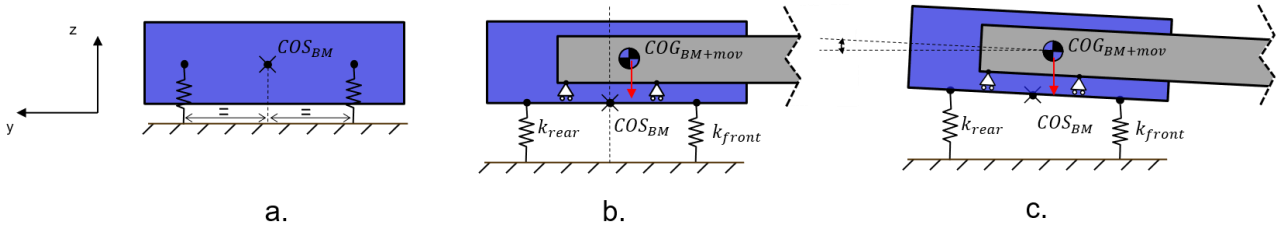

Figure 29. Side view of the mechanism with the location of COG.

Continuing with that reasoning, if the BM experiences an angle and the BM is free of stiffness and friction in Y direction, the BM will start moving in the positive Y direction, just due to the moment generated by the mass distribution. This effect is going to be called parasitic Y displacement of the BM or drift and it is accounted for by the BM motors, the contribution of this effect to the BM motors force is negligible.

Until this point, the BM is experiencing an angle in the neutral position due to the distance between the COG (BM + movers) and the Center of Stiffness (COS) of the BM guiding mechanism.

On top of this there is another effect on the BM motion. The variation of the support stiffness, as introduced in section 3.6. The compliant mechanism that guides the BM experiences a loss of stiffness along its stroke. This change in stiffness in Z direction (gravity) will generate a drop in the Z position of the BM when at the limit positions of the stroke. This drop will results in an arc shape motion of the balance in YZ plane as represented in Figure 30.

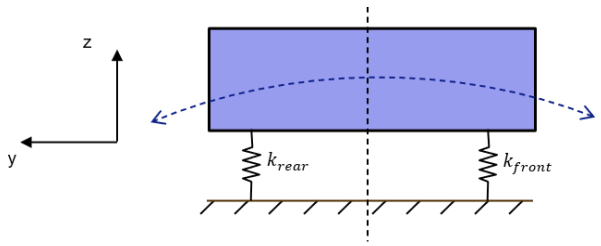

Figure 30. Arc shape motion of the BM.

Analyzing the limit positions along the motion of the BM (maximum operational stroke in both directions), it can be seen that the effects previously mentioned add up to increase the BM angle. In Figure 31 the limit positions of the BM and end effector can be seen.

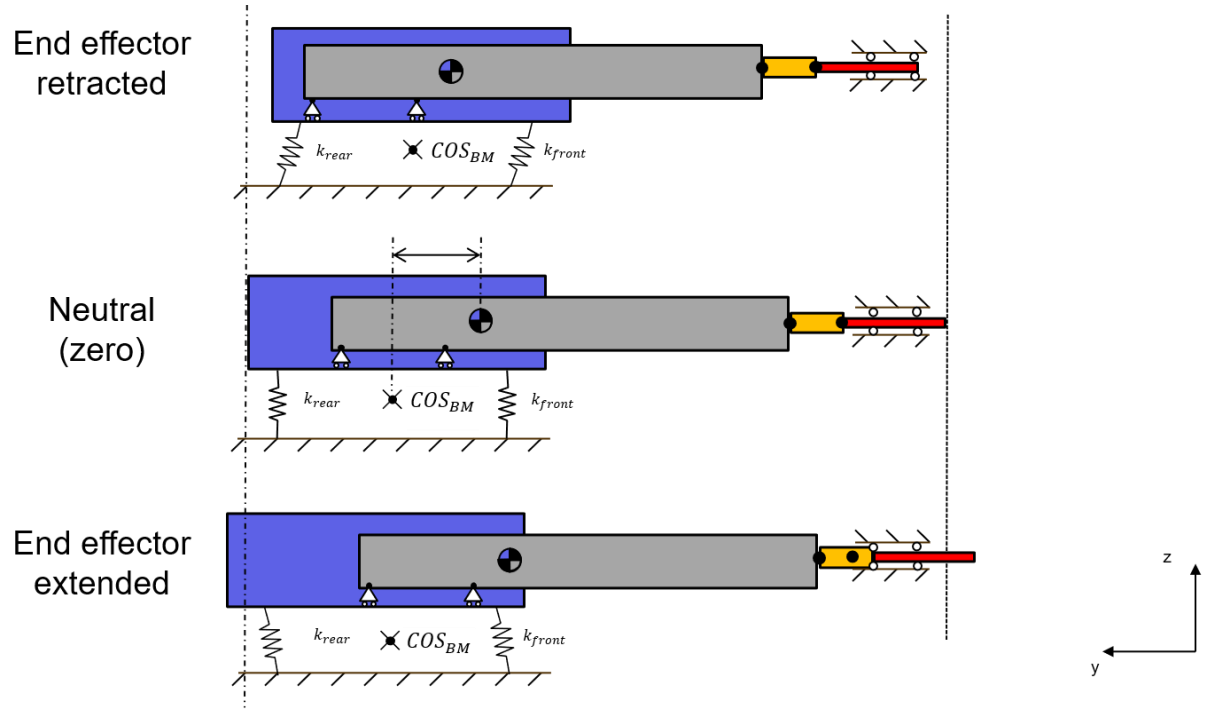

Figure 31. BM limit and neutral positions representation.

From the figure, it can be seen that when the end effectors are retracted, the BM is in the maximum (negative Y) stroke position and the distance between the COG of the movers and the COS of the BM guiding mechanism is minimum. On the other hand, when the end effectors are extended, the BM is in the maximum (positive Y) stroke and the distance from the COG of the movers to the COS of the BM guiding mechanism is maximum. That means that, in this situation, the front flexure has the highest load (more contribution of the movers' mass) and added to this, the BM is in a limit position, which means that the stiffness is the lowest. Both effects, more load and less stiffness add up and increase the BM angle.

In Figure 32, the effects of the Z drop of the BM and the angle around the X axis are represented. Due to the stiffness in Z, the BM will always experience a drop Z. Due to this drop, exaggerated in the representation, the end effector will experience a displacement in Y. Next to this, when the BM experiences an angle, the same effect happens, the end effector will be displaced in Y. The two effects happen at the same time.

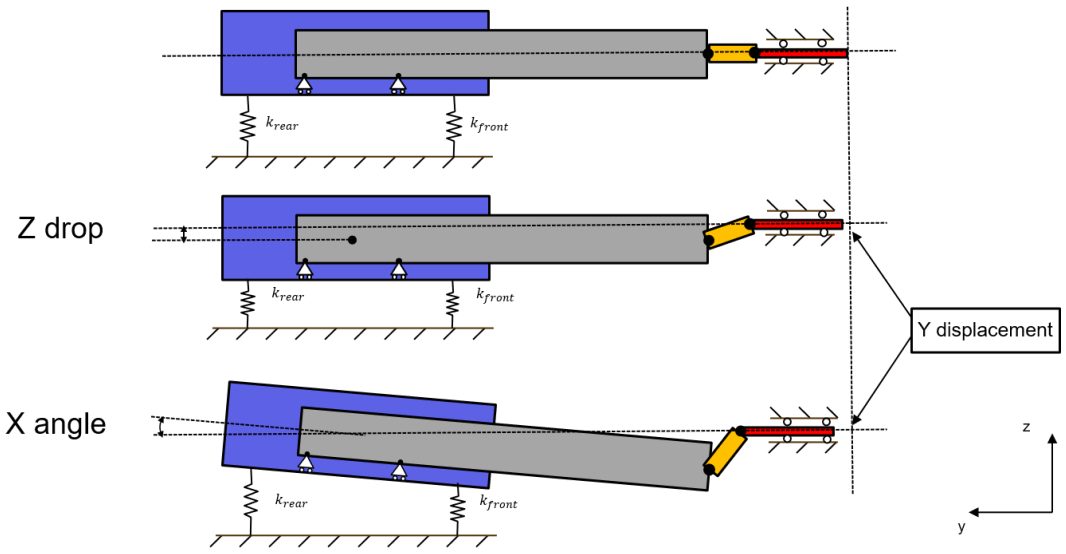

Figure 32. Representation of the BM angle effects on the system.

The function of the decoupler can be understood with this representation. If the decoupler was not present the Z drop of the BM and also the angle will affect the performance of the front cylindrical joint. However, the decoupler is a compliant mechanism that has certain rotational stiffness, thus, the loads in the front cylindrical joint will be affected by the previously mentioned effects.

The accuracy needed in the positioning of the end effectors is presented in Table 3 in section 9.1 (confidential). At the end of this section, the contribution of the BM angle to the Y error budget for the end effector will be presented.

In summary, the BM angle has effects on:

- BM parasitic displacement in Y (drift).
- Errors in the Y position of the end effector.
- Loads in the front cylindrical joint.
- Loads in the back cylindrical joint.
- Loads in the BM guiding mechanism.

Two paths are selected to study the effect on the BM angle: the first is the increase of the front flexure stiffness, which directly affects the position of the COS, and the second is the adjustment of the Y position of the movers COG. A representation of both cases can be seen in Figure 33.

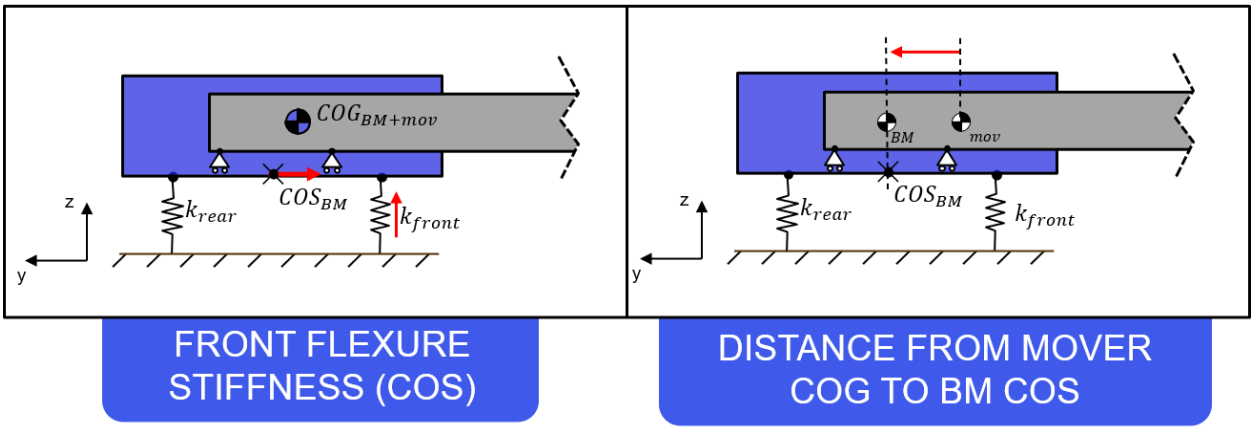

Figure 33. Case 1 and 2 for the study of the BM motion.

Starting with case 1, the increase of the front flexure stiffness, in Figure 34 the results from the analysis of the BM motion and angle due to this parameter are presented. In the left Y axis, the BM Z position, is linked to the red lines in the plot. In the right Y axis, the BM angle is represented and is linked to the blue lines in the plot. In the X axis, the BM Y stroke.

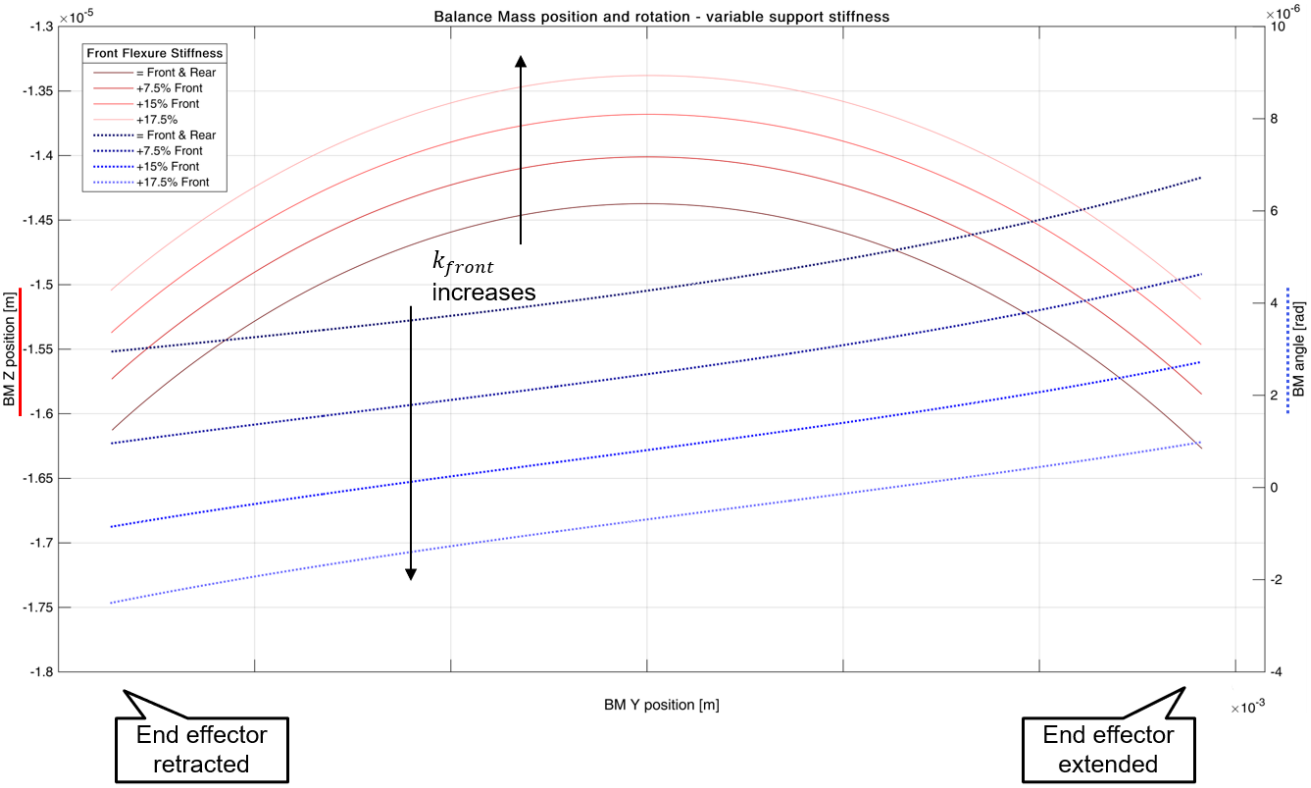

Figure 34. Balance mass position and rotation in YZ plane due to change of front flexure stiffness.

Starting the analysis with the BM Z position (left axis, red lines), the first thing that catches the attention is the arc shape motion of the BM due to the variable support stiffness. As the balance mass displaces from the zero position, it losses stiffness, thus it drops in Z direction. If the stiffness of the front flexure is increased, the drop is Z is reduced as there is a higher support load for the same mass.

Placing the focus on the BM angle (right axis, blue dotted lines), the angle is reduced as the front flexure stiffness is increased. Additionally, there is another effect to remark in the BM angle, it can be seen that the slope of the BM angle changes as the stroke changes (the slope is not constant). As a justification for this phenomena, Figure 35 is presented.

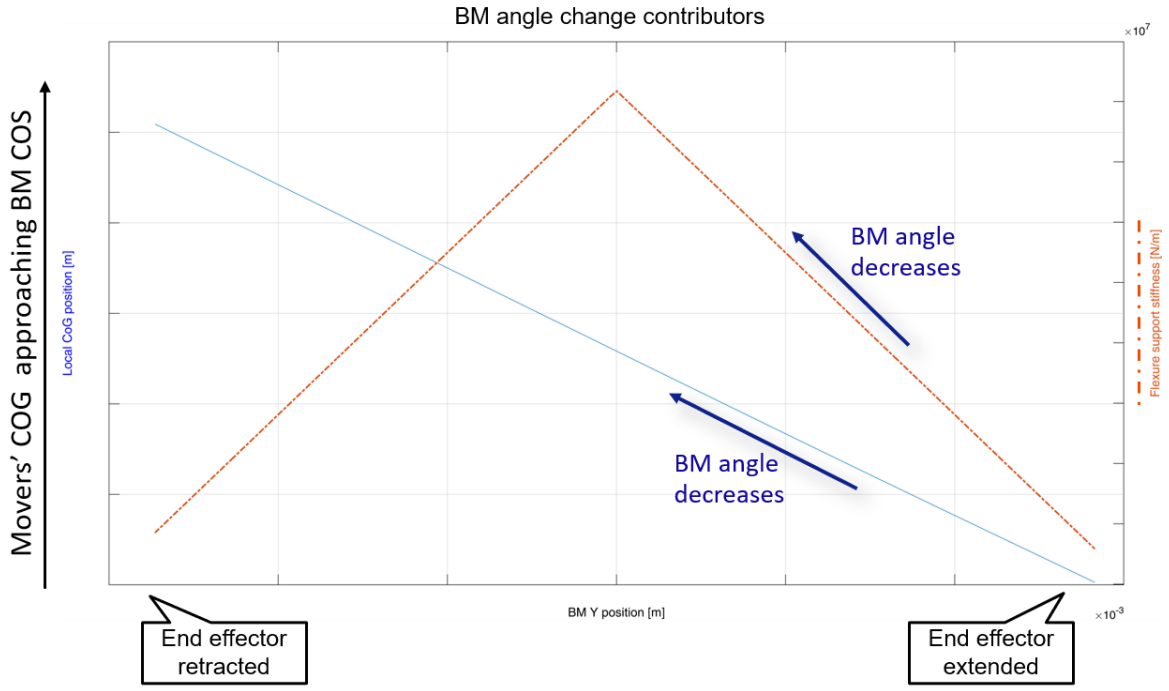

Figure 35. BM slope change justification.

In Figure 35, the flexure's stiffness (right Y axis) and the distance between the movers' COG and the BM COS (left Y axis) are plotted against the BM stroke. Starting from the end effector extended position, the distance between COG and COS is at its maximum and the stiffness of the BM as its minimum, thus the maximum angle (in accordance with Figure 34). As the BM approaches de zero position, the stiffness increases and the distance between COGs is reduced, that means both parameters are helping to reduce the BM angle. From the zero position to the negative BM stroke (end effector retracted) the stiffness starts decreasing again and the COG keeps getting closer, thus each effect is pointing in one direction (increase/decrease BM angle). Because of that, the slope of the BM angle changes and is different between one side of the stroke and the other (although not clearly visible in the plotted configuration).

In order to reach zero angle in the BM in its neutral position, the stiffness of the front flexure has to be 15% higher that the rear flexure stiffness, for this specific configuration. Nevertheless, the angle variation along the stroke cannot be avoided with this solution as it is due to the motion of the system. Reducing the angle in the neutral (zero) position, decreases the maximum angle to which the BM is subjected along its stroke and also the nominal Z drop that the BM will experience.

To continue with the analysis, the influence of the distance between the movers' COG and BM COS in the neutral position (zero BM stroke) has been studied and the results can be seen in Figure 36. The same axis representation holds for this plot.

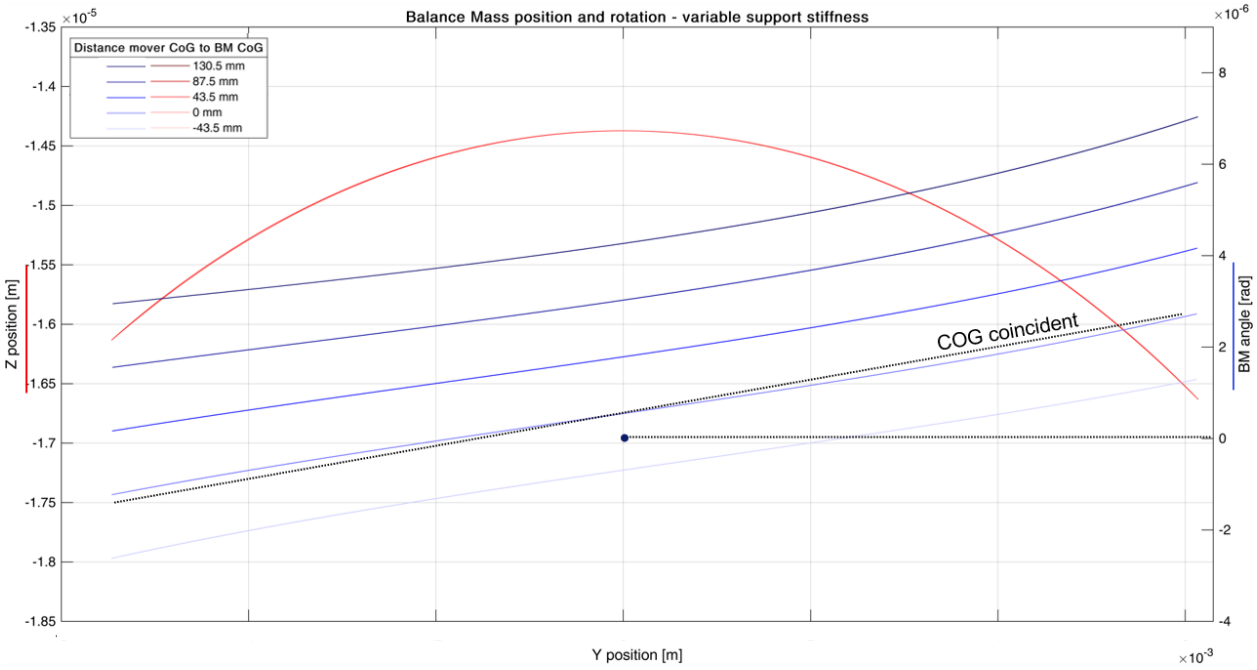

Figure 36. Effect of movers COG on BM angle and position.

The main difference from the previous analysis is that now, the change of position of the movers COG does not affect the Z drop of the BM. The BM angle is reduced as the COG of the movers is located closer to the Center of stiffness (COS) of the BM. Is this specific situation the COG of the BM is in line (same Y coordinate) with the COS. To give whole sense to this analysis, it should be clear that what makes the BM angle change is not the fact that the movers' COG is closer to the BM COG but to the BM COS. An important remark in this analysis is that the BM angle is not zero when the COG of the movers is coincident with the COG of the BM (dotted lines in Figure 36). This is due to the contribution of the pushrod, whose mass is split between the BM and the front cylindrical joint.

In summary, both analyses are focused on the distance between the COG and the COS. In case 1, the front flexure stiffness has been changed, thus changing the COS position to the front. In case 2, on the other hand, the COS remains in the same position but the COG has been changed to the back. In Figure 37, a detailed representation of the situation in which the BM angle is zero in the neutral position can be seen.

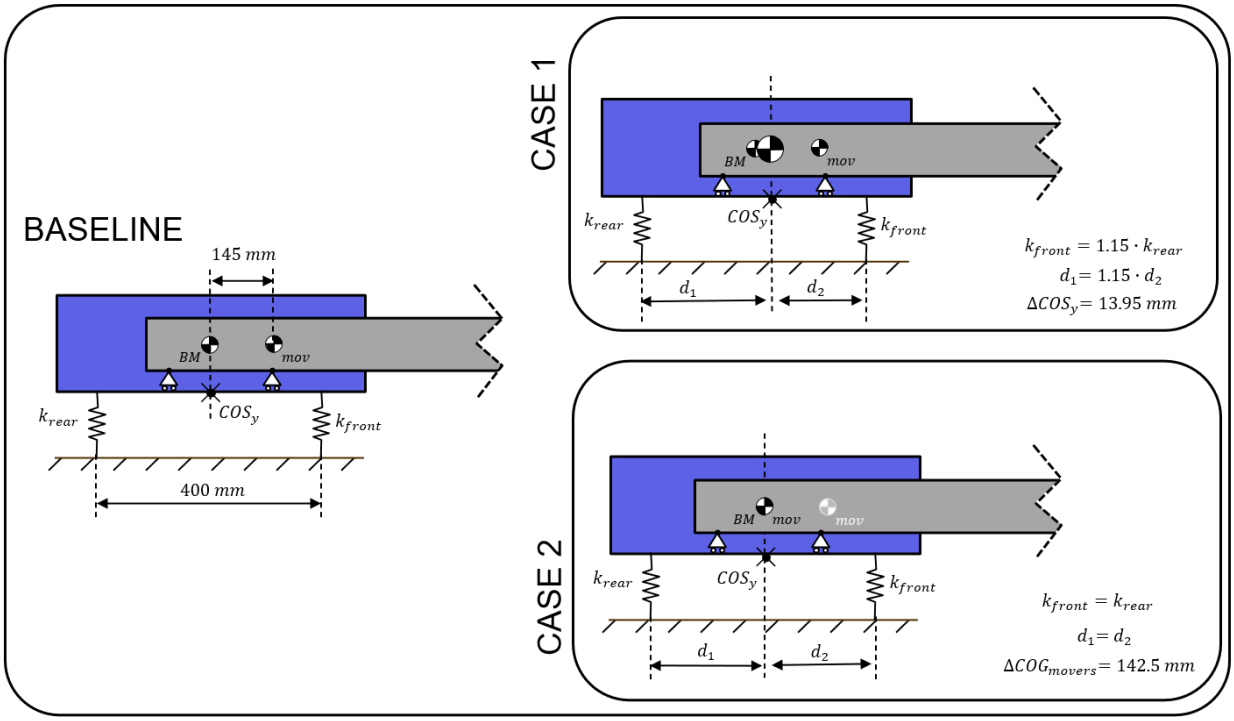

Figure 37. COG and COS positions for zero BM angle representation (Case 1 and Case 2).

In the baseline situation, the BM COG is in line with the flexures' COS. For case 1, the front flexure stiffness has to be 15% stiffer than the rear flexure for a zero BM angle. This generates a shift of the COS to the front. Considering this shift to be the same amount of the flexure stiffness (15%), the COS has shifted 13.95 mm to the front which should coincide with the combined COG of the movers and BM. A hand calculation has been made to prove that the combined COG of the movers and BM (plus a contribution from the movers) is at that position. The reference point for the distances of the COG is the original position of the BM COG.

$$COG_{mov\&BM} = \frac{m_{BM} \cdot y(COG_{BM}) + m_{mov} \cdot y(COG_{mov}) + \frac{m_{decoupler}}{2} \cdot y\left(COG_{pushrod}\right)}{m_{BM} + m_{mov} + \frac{m_{decoupler}}{2}} = 13.65\ mm$$

A small deviation exists due to the assumption that the decoupler contribute with half of its mass to the BM and the other half to the front cylindrical joint.

In the case 2 representation of Figure 37, it is shown that for the case 2 analysis, the COS remains in the same position and, in order to make the COG and the COS coincident, the movers' COG has been moved to the same position as the BM COG. However, in this position the BM is not exactly at a zero angle position due to the contribution from the decoupler.

Until this point, the BM angle has been introduced and its' effects explained. In the following subsection the effects of this angle into the exported reactions and end effector positioning will be analyzed.

5.2.1. Effect of BM angle on the exported reactions.

In Figure 32, a representation of the effects of the variable stiffness have been shown. The BM angle affects, at first sight, the exported reactions and the Y positioning of the end effector.

Starting with the effects in the BM guiding loads. Three cases are analyzed in this section, the first case, with a configuration in which the BM angle is zero in the zero stroke position and the decoupler stiffness is zero too. In the second case, the BM is in the baseline configuration (non-zero angle) and the decoupler stiffness still zero, and the third case, the BM is in the baseline configuration and the decoupler stiffness is not zero.

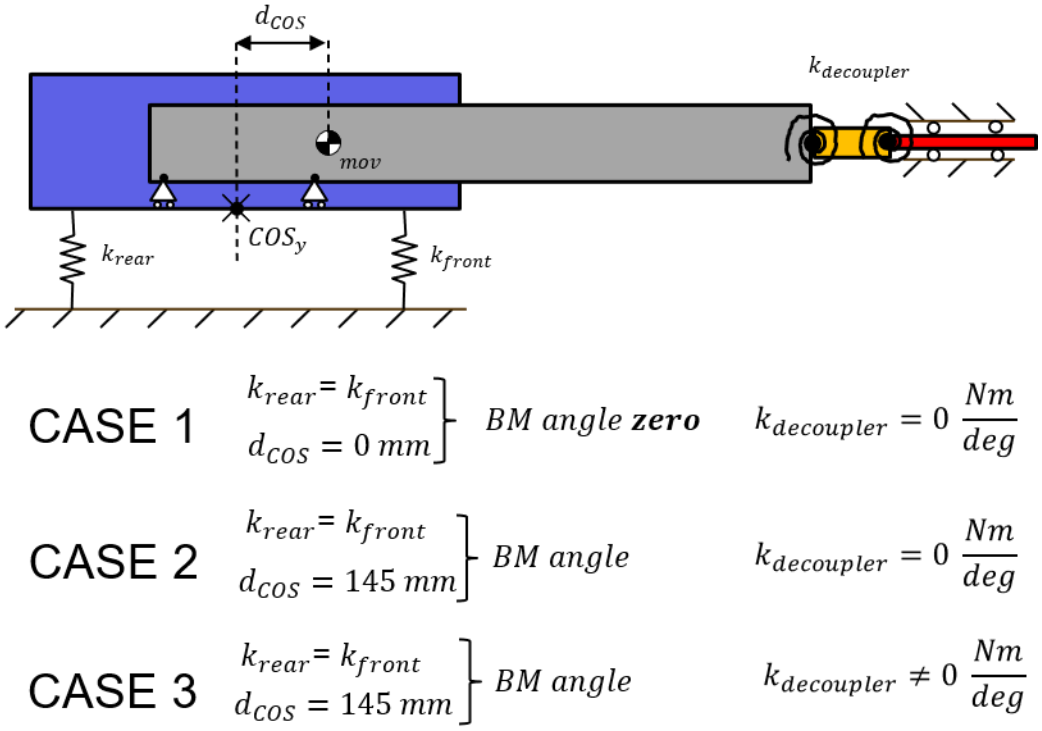

Figure 38. Cases to study the loads in the BM guiding mechanism.

Starting by the impact in the reaction forces, in Figure 39, the loads in the BM flexures along the stroke of the BM can be seen for the 3 cases previously introduced.

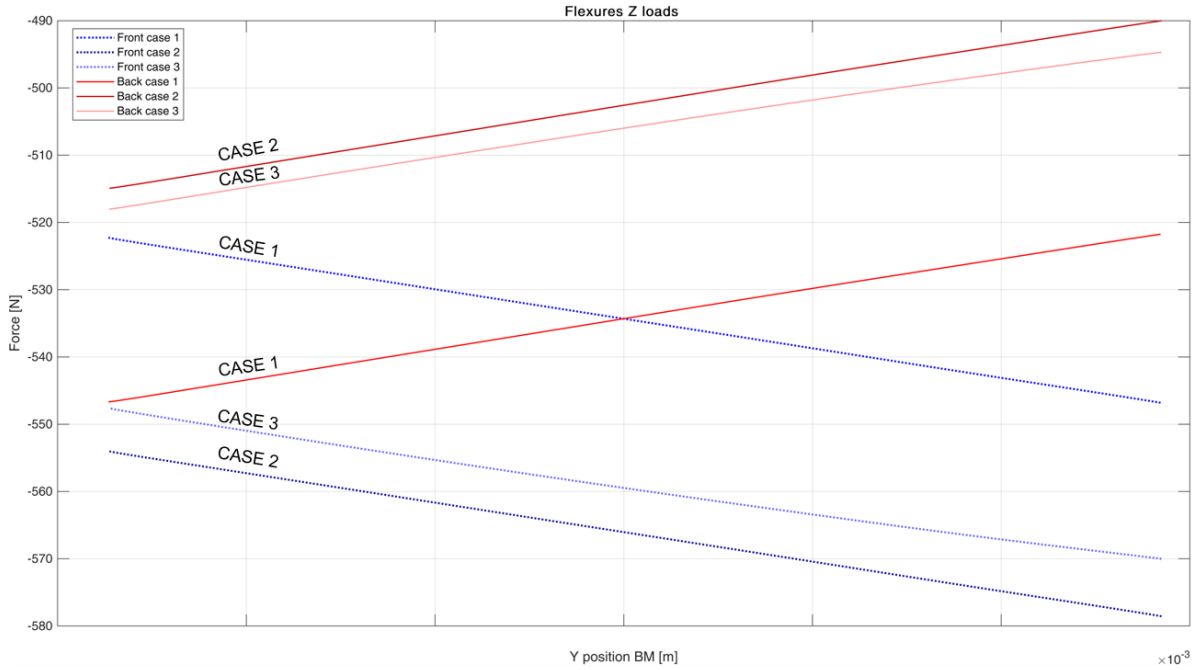

Figure 39. Z reaction loads in BM flexures.

In case 1, both flexures (front and back) experience the same load at the neutral (zero) position. When the angle increases, during movement, depending of the COG position with respect to the COS, the load is alternating between the front and the rear flexure but the total force (combination of all flexure loads) remains constant.

In case 2, the flexures never experience the same load (not crossing) because the angle of the BM is never zero. This will generate a constant moment in X to the REMA frame. Again the combination of the flexures remains constant.

In case 3, the behavior is the same as in case 2. However, the back flexure experiences a load increase and the front flexure a load decrease (Z loads are negative). As it can be seen the increase/decrease in both flexures is not the same amount. This will generate a slight increase in the total Z load in the BM due to the contribution of the decoupler stiffness which is trying to compensate for the BM angle. When the decoupler stiffness is added, the BM angle is reduced.

From this analysis, the carrying load difference between the 3 configurations can be seen and the flexures can be designed accordingly. The variation of the load during motion is of importance for life time analysis of the flexures (fatigue analysis). In case 3, for example, the front flexure will be subjected to a constant load of 565N, an alternating load of 13N (at 2.3Hz). In Figure 40, the alternating load on a front BM flexure can be seen.

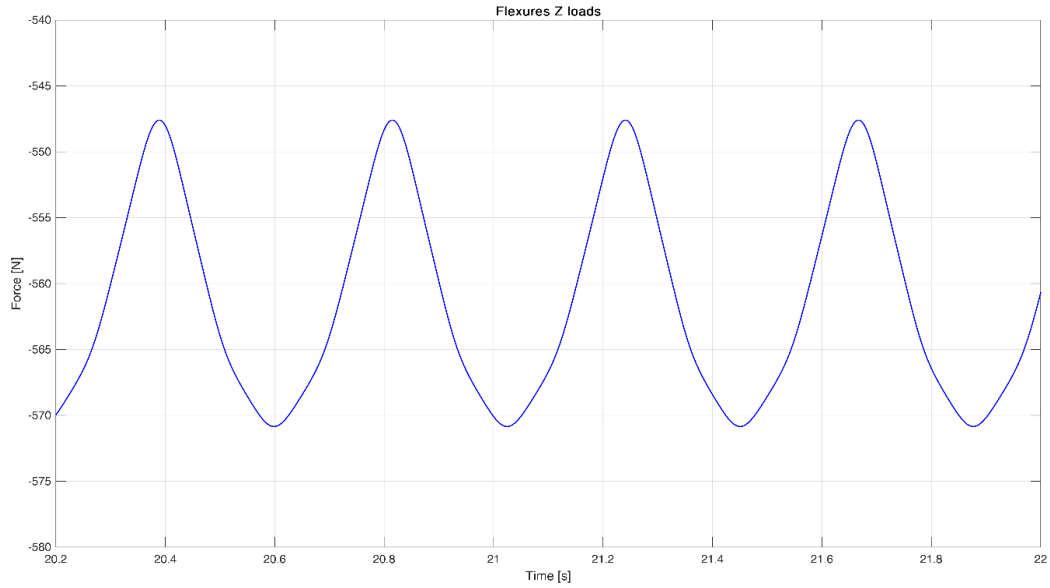

Figure 40. Loads on a BM flexure.

The same results are now shown for the loads in the front cylindrical joint for the same 3 cases presented in Figure 38. There is no different in Z force between case 1 and case 2, that means that the BM angle makes no difference in this load when the pushrod has zero stiffness and its value is purely due to the mass that this joint is supporting. However, in case 3, when stiffness is added to the pushrod, the Z force increases and varies along the stroke. The variation along the stoke is due to the BM angle and thus pushrod hinge angle change during motion.

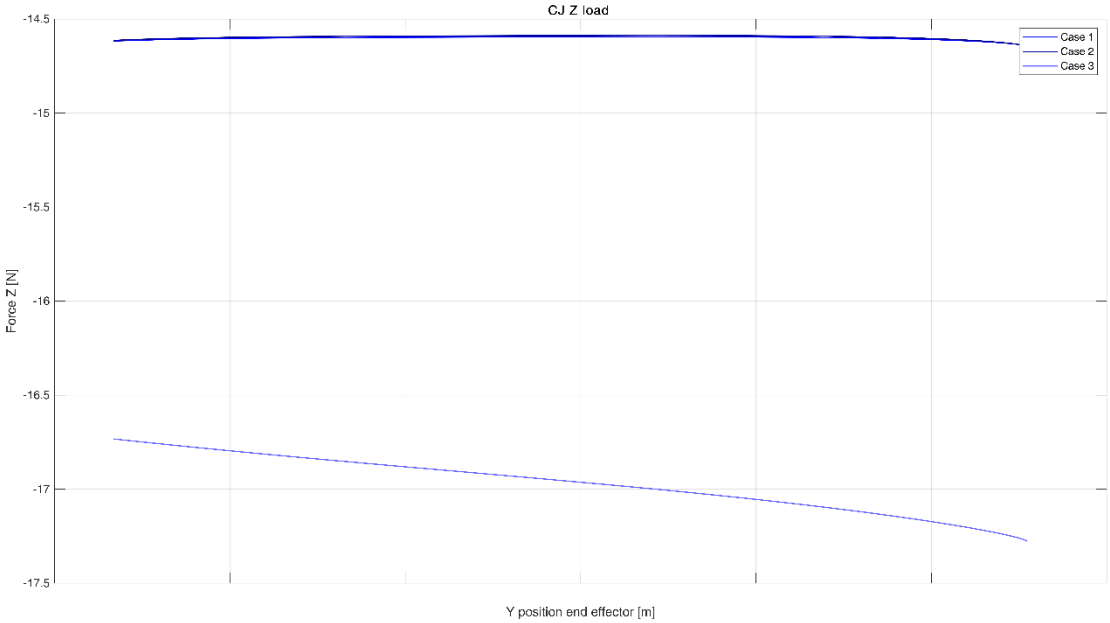

Figure 41. Z load on front cylindrical joint.

In Figure 42, the reactions to the force frame measured in the Point of Interest (PoI) are presented. This case is not including the stiffness in the moving direction (Y) and thus is not comparable with Figure 26. The Y stiffness is not included because the analysis was focused just on the influence of the BM angle, to avoid the influence of other effects.

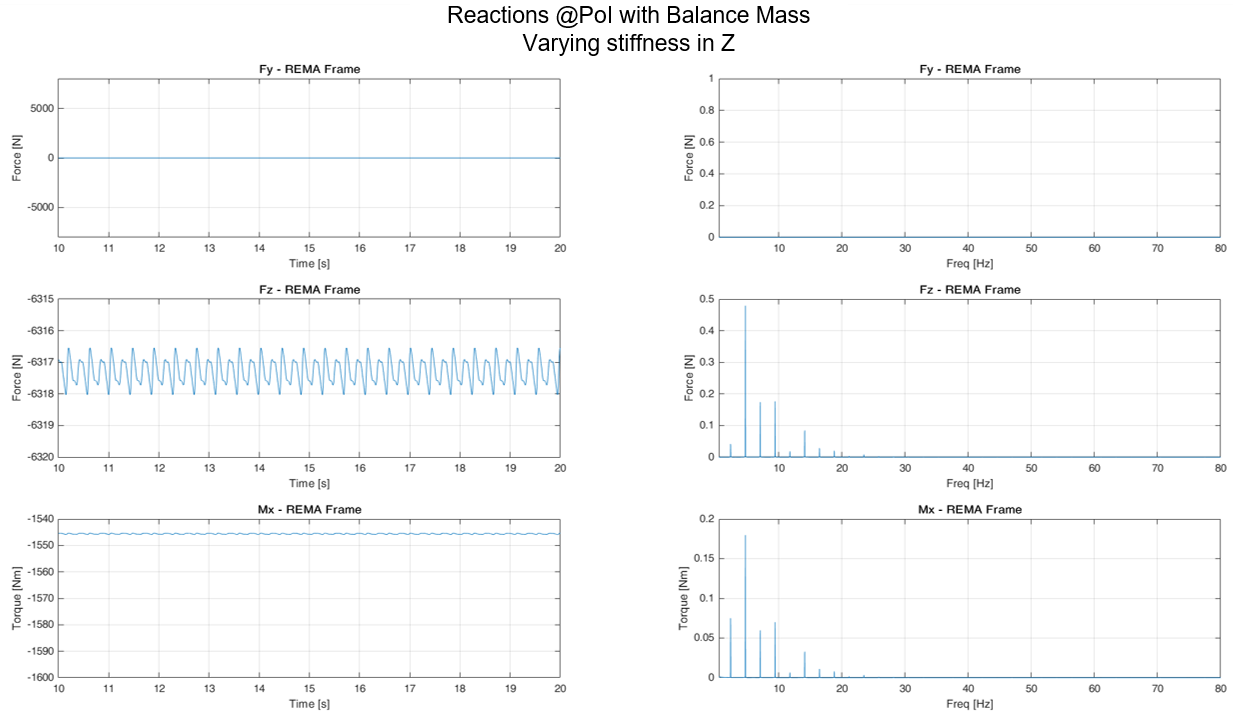

Figure 42. Reactions to the force frame with BM angle.

Firstly, it can be seen that it has no effect in the Y reaction force. Secondly, in the Z reaction it does have an effect, as expected. However, the effect on the total reaction load just because of the variation of the BM guiding mechanism stiffness is not significant. It is a 1% of the total allowed reaction load in Z for the low frequency range. The same holds for the moment in X, which is comparable to the one shown in the ideal BM case (Figure 25).

To conclude, both stiffness in Y and Z are combined and the exported reactions are shown in Figure 43.

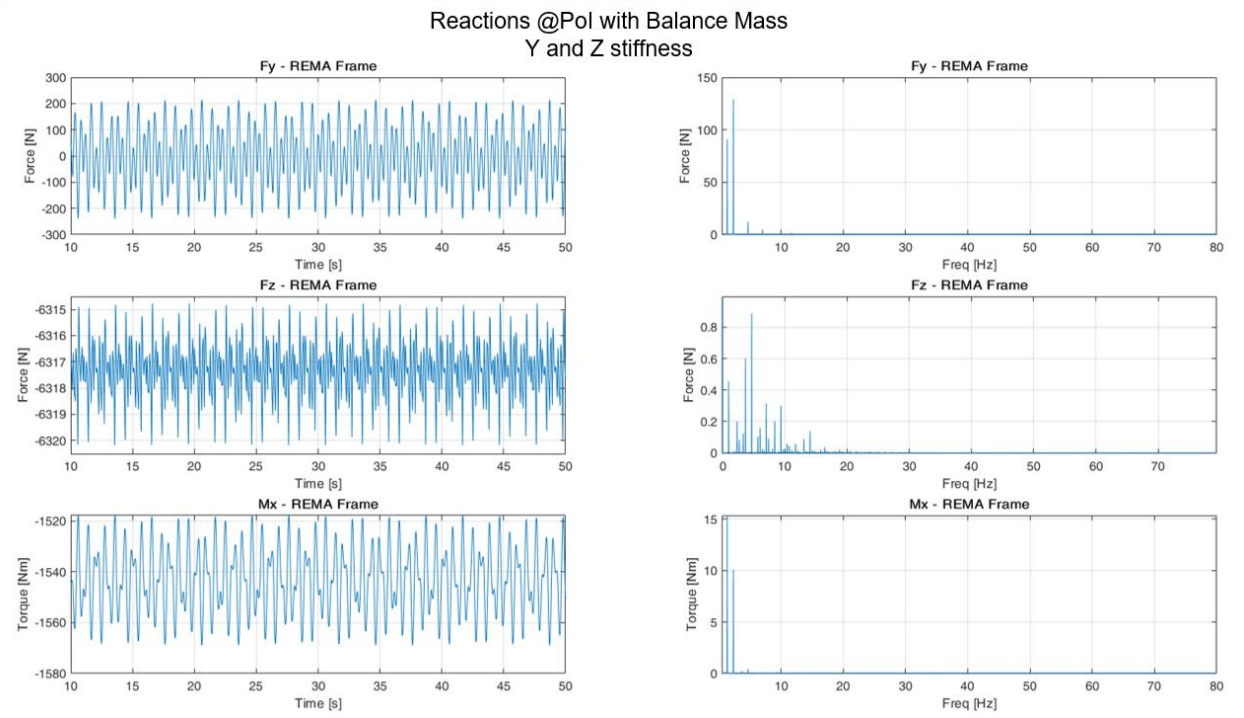

Figure 43. Reactions to the force frame combining Y and Z stiffness.

Figure 43 is combining the cases studied in Figure 26 (case in which the Y stiffness was added to an ideal BM guiding mechanism) and Figure 42 (case in which the BM had a drop in Z direction). In the results it can be seen that both effects affect the Z reaction load while the Z reaction and the X torque remain as in Figure 26.

In this section, the effects on the local (BM flexure and front cylindrical joint) and global reaction loads due to the BM angle have been analyzed. I has been seen that the BM angle has several effects on different part of the mechanism. All the results presented are for the studied configuration, as mentioned in previous sections, this analysis has been performed with a specific motion profile out of thousands. The summary of the results are:

1. The flexures of the BM guiding mechanism experience a Z load variation of $\pm 13N$ due to the change in BM angle.
2. The front cylindrical joint experiences an increase of $3N$ in Z load due to the BM angle.
3. The front flexure stiffness has to be 15% higher than the rear for the BM angle to be zero in the neutral position.
4. The mover's COG has to be displaced $\sim 150\,mm$ for the BM angle to be zero in the neutral position.
5. The BM angle and Z drop has a contribution of 1% to the Z load budget in the low frequency range for the studied configuration.

In the next subsection, the influence in the end effector positioning will be presented.

5.2.2. Effect of BM angle on end effector positioning.

Apart from the effect on the loads in the BM flexures, the BM angle also generated a parasitic Y displacement in the end effector, as presented in Figure 32. The end effector have a specification for the position in Y direction, stated in Table 3 (confidential). In this subsection, the Y displacement of the end effector has been analyzed for different BM suspension stiffnesses. The Z stiffness of the BM directly affects the drop of the BM and thus, it influences the position of the end effector.

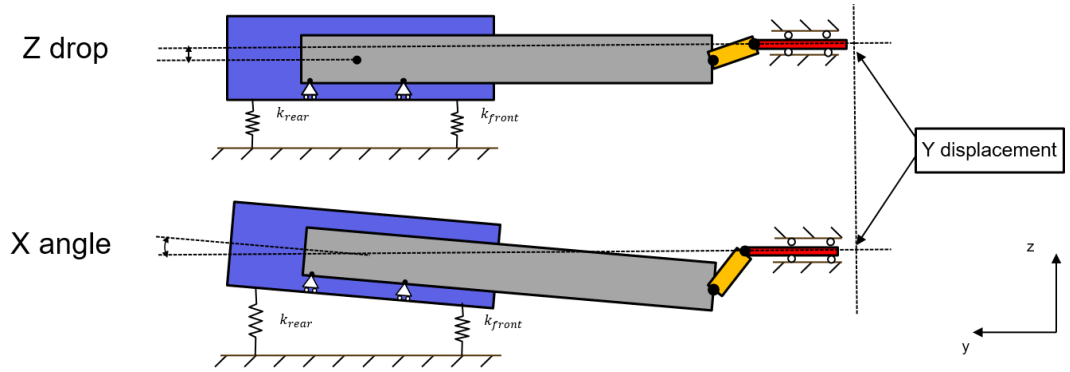

Figure 44. Y parasitic displacement in end effector.

In Figure 45, the Y parasitic displacements are presented in both the maximum stroke position and the neutral (zero stroke) position for the Y0 end effector.

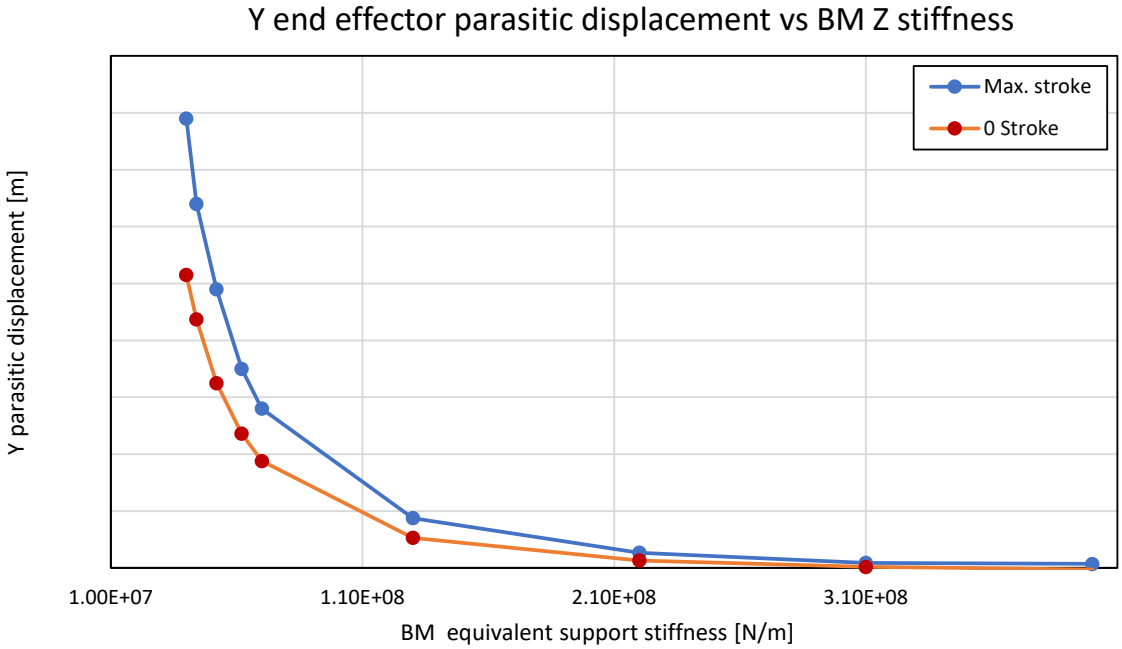

Figure 45. End effector Y displacement vs BM support stiffness.

From Figure 45, the calculated maximum parasitic Y displacement of the end effector (softest stiffness analyzed) corresponds to a **0.01 %** contribution to the total allowable error in the Y positioning of the end effector and thus it is considered insignificant on its own. A good remark to make here is that this analysis is focused on a disturbance analysis in the YZ plane of the mechanism.

However, the same phenomena can be applied to the XY plane. In that case, a misalignment between the COS and COG (Figure 46) could induce a BM angle around the Z axis. This additional BM angle around the X axis will also generate a parasitic Y displacement of the end effector that will add up to the one just calculated.

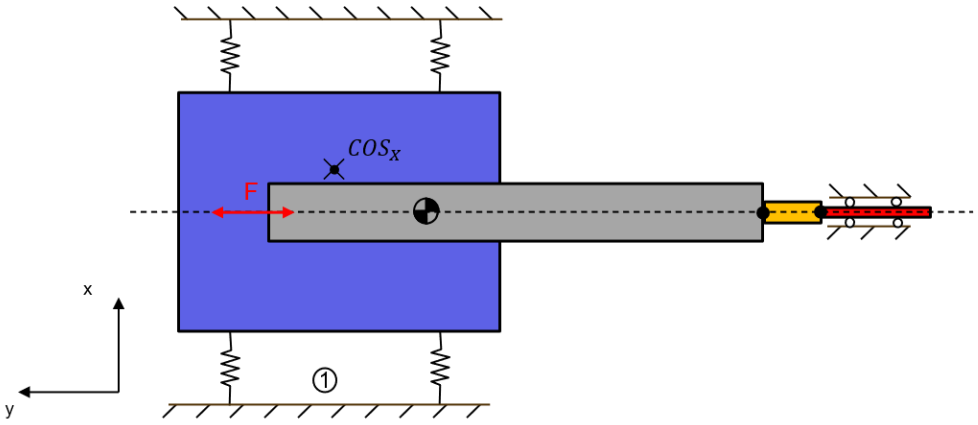

Figure 46. Possible disturbance in YX plane (COS misalignment).

Despite the fact that the error in the positioning of the end effector is considered negligible, if the specification is tighten, it could become a problem. In order to avoid this disturbance to affect the position of the end effector, the control system be aware of this disturbance. In Figure 47, two position of the encoder are shown (green boxes).

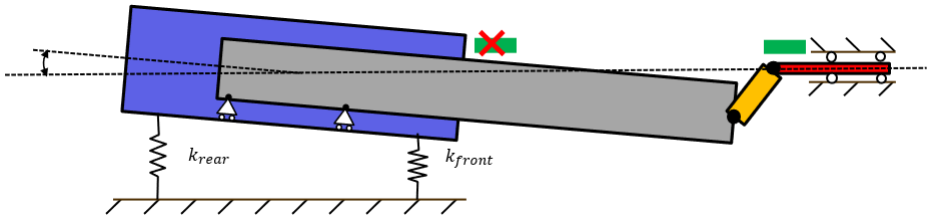

Figure 47. Encoder position.

Thus, the encoder should be located somewhere after the decoupler to take into account the positioning error generated by the BM angle. If the encoder is placed before the pushrod, the effect of the BM angle in the positioning of the end effector will be unknown for the control system.

6. Conclusions.

This thesis made it possible to detect discipline specific design parameters that affect a top level specification, by the use of a conceptual multi-body model-based approach. This approach aimed to tackle and avoid possible specification issues at a later development stage, by modeling and analyzing an abstract version of the current system in an early stage of the design process. Multibody model-based approach is a powerful alternative when working with complex mechatronic mechanisms because of its power to locate relevant effects in an early design stage.

By analyzing the model, several disturbances have been detected that have an impact on the top level specification. The multi-disciplinary nature of these disturbances helped to raise awareness of the importance of the communication between disciplines into the fulfillment of a specific requirement.

The first analysis was to evaluate the conceptual need of a balance mass in the system. It has been concluded that for a system without balance mass, the moving mass of the mechanism has to be lower than 500 grams, which for this mechanism was concluded to be infeasible. When a balance mass is included in the system, extra attention should be paid to the definition of the mass, the allowed stroke and the stiffness in moving direction.

Going more in depth, the analysis of the mass distribution of the system combined with the non-linear support stiffness of its guiding system, led to the discovery of five different inputs for the design of the module. The relative center of gravity position of the movers with respect to the BM appears to create an undesired angle in the BM. Combined with the non-linear support stiffness of the balance mass during motion, this generates an angle variation of $3\ to\ 10\ \mu rad$. This effect is translated to a flexure load variation in the balance mass guiding mechanism up to $90\ N$ between front and rear flexures, which at the same time has a sinusoidal variation due to the change of stiffness along the stroke of $13\ N$. From this analysis, an increase in the front flexure stiffness of 15% compared to the rear is needed to minimize the BM angle (input 1). Moreover, the effects on the flexure loads can be used as input for flexure fatigue requirements (input 2). The angle created in the BM due to the mass distribution generates a non-desired displacement of the whole BM, which has to be controlled by the additional BM actuators (input 3). As another solution to minimize the BM angle, the mass distribution in the BM can be adjusted by tuning the mover's COG position. A delta of $\sim 150\ mm$ with respect to the current COG position is needed (input 4). Finally, as the balance mass is linked to the end effector, the angle generated impacts its positioning, generating an error of $9\ nm$ in Y (input 5).

This approach has been applied to an early-conceptual stage and thus is not comparable to the current methodology which is used in detailed-design phase. Despite being located in different design stages, the fact that non-linear effects cannot be included in the current methodology, makes this approach a good alternative to analyze the influence of the possible non-linear effects in the whole system.

My personal opinion about the approach followed is that it has given a good insight in the current design as well as the discovery and quantitative analysis of several phenomena that were unknown. The approach helps to understand complex phenomena in a really simple and visual way, which facilitates the understanding and thus a better decision making. In my opinion there should be a continuation in this line of work with the undermentioned recommendations to back up and guide the future REMA development.

7. Future work.

In this section, the next steps that could follow this project will be explained. Once the model for the system is set up, several analyses can be performed. In this project, an abstracted version of a REMA concept has been modelled. However, due to time reasons not all the desired analyses have been performed. The initial proposal for the project was to analyze the current system and propose new concepts to analyze them via the same procedure.

- As shown in the expected V model in section 2.1 in Figure 9, the project should have continued with the generation of strategies to follow the detected sub-system specifications from the *"current system analysis"*. After the strategies are defined, new concepts are proposed and conceptually modeled via the multibody model. Finally a new concept is proposed for the start of the detailed analysis.

- An experiment could be set up to validate the current model. A draft idea of what the experiment should look like to represent the current model is described here. The experiment needs to contain at least: a balance mass with a flexure-like guiding system, two movers with its actuators and guiding system, and two end effectors. The experiment should have the capability to at least: adjust the mass of the Balance mass (preferably maintaining the COG position), adjust the Y position of the movers' COG (as in the analysis), activate and deactivate the Balance Mass, and make the BM stiffness in the moving direction adjustable between zero and a non-zero value.

  For the measurements: a gyroscope could be installed in the BM, and a position measuring device in the end effectors and two of the flexures of the BM guiding system. The mechanism should be excited with the same motion input as in the model, to have comparable frequency content. Finally, the same experiments performed in the model could be performed with this experiment. By comparing the results from the BM angle, end effector position and BM drop in Z between model and experiment, the differences between both results will be quantified.

- The analyses performed during this project have been mostly focused on the effects in the YZ plane while there are other relevant disturbances that cannot be caught in this plane. The disturbance generated by the misalignment of the actuators, or the BM angle due to a misalignment in the COS of the BM guiding mechanism are some of them.

- About the positioning of the end effectors, the current model does not allow to evaluate the errors in the Z position. This is due to the simplification in the use of prismatic joints to model the front joint connection. This joint has an infinitely stiff constraint in the radial direction and thus nor Z neither X displacement will occur. It will be valuable to model this joint with another approach to be able to measure this positioning error.

- Moreover, the software allows to interact between different disciplines and to link the multi-body model to other Simulink modules. During the analysis it has been noticed that some effects like, for example, the drift of the balance mass, limits the analysis of the exported forces and cannot be avoided without the addition of a control system. The implementation of a simple control system to control the position of the BM will be a valuable implementation.

- As mentioned in the assumptions section, the current analysis has been performed with the assumption of rigid bodies. It is known that in reality, the stiffness of the solid bodies plays an important role in the dynamics of the mechanism. The software allows to introduce several approaches to model the flexibility solid bodies. In order to define an specification for the stiffness of some parts of the mechanism, this should be considered as future work.

8. Bibliography

Eigner, M., Gilz, T., & Zafirov, R. (2012). *Interdisziplinäre Produktentwicklung - Modellbasiertes Systems.* Technische Universität Kaiserslautern.

Graessler, I., Hentze, J., & Bruckmann, T. (2018). V-Models for interdisciplinary systems engineering. *International design conference - design* , (pp. 747 -756).

Hopkins, J. B., & Culpepper, M. L. (2009). *Synthesis of multi-degree of freedom, parallel flexure system concepts via Freedom and Constraint Topology (FACT) – Part I & II.* Elsevier.

Miller, S., Soares, T., Van Weddingen, Y., & Wendlandt, J. (n.d.). *Modeling Flexible Bodies with Simscape Multibody Software.* MathWorks.

Simscape, M. (2021). *User's Guide.*

Soemers, H. (2017). *Design principles for precision mechanisms.*

van der Wijk, V., & Herder, J. L. (2009). *Guidelines for low lass and low inertia dynamic balancing of mechanisms.*

van der Wijk, V., Herder, J. L., & Demeulenaere, B. (2015). *Comparison of various dynamic balancing principles regarding additional mass and additional inertia.*

Zhang, D., & Wei, B. (n.d.). Dynamic balancing of mechanisms and synthesizing of parallel robots. Springer.